 Click here to view linked References

Lipid transfer proteins and a PI 4-kinase initiate nuclear phosphoinositide signaling

Noah D. Carrillo[1,2,4], Mo Chen[1,3,4], Tianmu Wen[1], Poorwa Awasthi[1], Trevor J. Wolfe[1], Vincent L. Cryns[1,2,5,*] and Richard A. Anderson[1,5,*]

[1]University of Wisconsin Carbone Cancer Center, University of Wisconsin-Madison, School of Medicine and Public Health; 1111 Highland Avenue, Madison, WI 53705, USA
[2]Department of Medicine, University of Wisconsin-Madison, School of Medicine and Public Health; 1111 Highland Avenue, Madison, WI 53705, USA
[3]Current Address: Department of Pharmacology, Joint Laboratory of Guangdong-Hong Kong Universities for Vascular Homeostasis and Diseases, School of Medicine, Southern University of Science and Technology, Shenzhen 518055, China
[4]Co-first authors
[5]These authors contributed equally to this work
[*]Correspondence: vlcryns@medicine.wisc.edu; raanders@wisc.edu

Summary 150 max

Phosphoinositide (PIP_n) messengers are present in non-membranous regions of nuclei, where they are assembled into a phosphatidylinositol (PI) 3-kinase (PI3K)/Akt pathway that is distinct from the cytosolic membrane-localized pathway. In the nuclear pathway, PI kinases/phosphatases bind the p53 tumor suppressor protein (wild-type and mutant) to generate p53-PIP_n complexes that regulate Akt activation. However, this pathway is dependent on poorly characterized nuclear PIP_n pools. Here we report that PI transfer proteins (PITPs), which transport PI between membranes to enable membrane-localized PIP_n synthesis, accumulate in the nucleoplasm in response to stress and supply nuclear PIP_n pools. PITPα/β and the PI 4-kinase PI4KIIα bind p53 and are required to generate p53-PI4P, which is further phosphorylated to synthesize p53-PIP_n complexes that regulate nuclear Akt activation and stress-resistance. Remarkably, PITPα/β and PI4KIIα initiate PIP_n-linkage to multiple proteins that are detectable by immunoblotting and [^{3}H]*myo*-inositol metabolic labeling and are resistant to denaturation, suggesting a posttranslational modification.

Key words

Phosphoinositide; phosphatidylinositol transfer protein; PIP_n-linked proteins, p53; PI4,5P_2; PI3,4,5P_3; nucleus; cell stress; Akt

In brief

Phosphatidylinositol transfer proteins initiate the nuclear PIP_n-linked protein network in membrane-free regions.

Main text

Phosphoinositide (PIP_n) lipids are synthesized from phosphatidylinositol (PI) in membranes by PIP kinases to produce a second messenger network comprised of seven distinct PIP_n isomers that play key roles in many cellular pathways[1]. Cytosolic class I PI 3-kinases (PI3Ks) catalyze the synthesis of PI3,4,5P_3, which leads to the recruitment and activation of the serine/threonine kinases phosphoinositide-dependent kinase 1 (PDK1), mTOR Complex 2 (mTORC2), and Akt at membranes[2-8]. Akt in turn phosphorylates many substrates, such as forkhead box O (FOXO) proteins, tuberous sclerosis complex 2 (TSC2), and BCL2-associated agonist of cell death (BAD), to promote cell growth and inhibit apoptosis[4]. This membrane-localized PI3K/Akt pathway is often hyperactivated in cancer and class I PI3K inhibitors are currently in the clinic[9, 10].

Akt is also activated in the nucleus[11-16]. Recent studies have identified a non-membranous nuclear PI3K/Akt pathway that is dependent on p53[17, 18], a tumor suppressor that is frequently mutated in cancer, resulting in gain-of-function oncogenic acitivities[19, 20]. In this nuclear pathway, wild-type and mutant p53 are sequentially modified by PIP_ns and their associated PIP kinases/phosphatases. The PI4P 5-kinase (PIPKIα) directly interacts with p53 and generates the p53-PI4,5P_2 complex (p53-PIP_n signalosome) in response to stress[18]. PI5P4Kβ has also been functionally linked to p53 as deletion of both genes is lethal in mice, but the mechanism is less defined[21]. The nuclear PI 3-kinase IPMK acts on p53-PI4,5P_2 to synthesize p53-PI3,4,5P_3 complexes, which then recruit and activate Akt in the non-membranous nucleoplasm[17, 18]. The nuclear

Akt pathway is insensitive to PI3K inhibitors currently in the clinic[17], highlighting its therapeutic importance.

Although multiple PIP_ns and PIP kinases/phosphatases are present in the nucleoplasm[16, 22-24], the mechanism by which the pool of nuclear PIP_ns is established and their molecular characteristics are unknown. Unlike the most abundant nuclear phospholipid, phosphatidylcholine (PC), which is synthesized *in situ* in the nucleus[25-27], PI represents a minor fraction of free nuclear phospholipids and is synthesized in the endoplasmic reticulum (ER)[28] that is contiguous with the nuclear envelope[29], suggesting that PI is transported into the nucleoplasm. In the cytosol, PI is transported from the ER to membranes and between membranes by a family of lipid transfer proteins, the phosphatidylinositol transfer proteins (PITPs). To date, PITPs have not been demonstrated in nuclear transport or any nuclear function. Intriguingly, PITPβ was reported to interact with p53 in a proteomics screen[30], prompting us to investigate a potential functional role for PITPs in regulating the synthesis of p53-PIP_n complexes and nuclear PIP_n signaling. Here we demonstrate that a subset of the PITP family is specifically required to generate the non-membranous nuclear PIP_n pools by transporting PI into the nucleus. Strikingly, the PIP_ns in these nuclear pools are coupled to proteins. Within this PIP_n pool, PITPs and the PI 4-kinase PI4KIIα bind p53 and initiate nuclear p53-PIP_n signaling, culminating in nuclear Akt activation and stress-resistance. These findings provide the first model for how PITPs regulate nuclear PIP_n signaling.

The nuclear localization of PITPs is regulated by cellular stress

The PITP family is composed of five members that are subdivided into two classes that exchange PI for PC (Class I, the single domain PITPα and PITPβ isoforms) or PI for phosphatidic acid (PA) (Class II, the single domain PITP cytoplasmic 1 (PITPNC1) and multi-domain PITP membrane associated 1 (PITPNM1), and PITP membrane associated 2 (PITPNM2) isoforms with C-terminal extensions)[31] (Fig. 1a). The most homologous members within the PITP family, PITPα/β/NC1, were expressed in the nucleus under basal conditions, and the nuclear levels of each isoform and PI4,5P_2 were increased by cisplatin as determined by immunofluorescence (IF) (Fig. 1b,c and Extended Data Fig. 1a). Confocal 3D sectioning (Extended Data Fig. 1b-e) confirmed the enhanced nuclear levels of PITPα/β in response to genotoxic stress, which were observed in all cell lines tested regardless of tissue of origin or p53 mutational status (Fig. 1d and Extended Data Fig. 2a). Multiple cellular stressors (genotoxic, oxidative and ferroptotic) increased the nuclear levels of PITPα/β, indicating a fundamental nuclear role for the PITPs in the cellular stress-response (Fig. 1e,f and Extended Data Fig. 2b). Moreover, cell stress induced the targeting of PITPs to the non-membranous nucleoplasm in all cell lines examined (Fig. 1g and Extended Data Fig. 2c and 3a-d).

PITPs regulate the nuclear PIP_n pool

All PIP_n isomers except PI3,5P_2 have been detected in the nucleus by multiple methods[16-18, 22, 23, 27, 32]. Among these, PI4,5P_2 forms distinctive nuclear foci that colocalize with nuclear speckle markers in regions devoid of membranes[16-18, 23, 33]. PI is the precursor of all PIP_ns[34] and together with our observation that cellular stress induces the nuclear localization of PITPs, we investigated the role of PITPs in regulating the nuclear PIP_n pool.

Silencing PITPα or PITPβ reduced basal and stress-induced nuclear PI4,5P_2 levels, while combined knockdown (KD) of both PITPα and PITPβ further decreased nuclear PI4,5P_2 levels compared to the individual KD (Fig. 2a,b). In contrast, PITPNC1 KD had no effect on basal nuclear PI4,5P_2 levels and minimal effect on stress-induced PI4,5P_2 levels (Fig. 2a,b). Combined KD of PITPα and PITPβ also suppressed stress-induced nuclear levels of PI4P and PI3,4,5P_3 (Fig. 2c,d). Combined KD of PITPα and PITPβ robustly inhibited stress-induced nuclear PI4,5P_2 generation in transformed and untransformed cells independent of p53 mutational status (Fig. 2e-g and Extended Data Fig. 3e). These results demonstrate that PITPs are necessary to generate the nuclear PIP_n pools that are detected by specific PIP_n antibodies (Fig. 2h).

PITPα/β bind p53 and their interaction is regulated by cellular stress

Together with the reported interaction of PITPβ and p53[30], the role of PITPs in regulating nuclear PIP_n levels suggest PITPs may play a functional role in generating nuclear p53-PIP_n complexes. To explore this, we investigated the interaction of p53 with all five PITPs using multiple approaches. Proximity ligation assay (PLA)[32] demonstrated class I PITPs (PITPα and PITPβ), but not class II PITPs (PITPNCI, PITPNM1 and PITPNM2), associated with mutant p53 ($p53^{mt}$) and wild-type p53 ($p53^{wt}$) in the nucleus, and that their association was enhanced by cisplatin (Fig. 3a,b and Extended Data Fig. 4a-c). Notably, the association of PITPα/β with $p53^{wt}$ was minimal under basal conditions and dramatically increased by stress, while PITPα/β associated constitutively with $p53^{mt}$ with a modest increase in response to stress. Like the nuclear localization of PITPs (Fig. 1g, Extended Data Fig. 1a-e and Extended Data Fig. 3a-d), the PITPα/β-p53 PLA complexes

were present in the nucleoplasm in regions distinct from the nuclear envelope (Fig. 3c, Extended Data Fig. 4d-f, and Supplementary Video 1-2).

The PITPα/β-p53 complex was next examined by immunoprecipitation (IP). Consistent with the PLA data, class I, but not class II PITPs, bound $p53^{wt}$ and $p53^{mt}$, and these interactions were increased by stress in all cell lines examined (Fig. 3d-f, h-i and Extended Data Fig. 5a,b,e-n). Although nuclear levels of PITPα/β and PITPNC1 increased in response to stress (Fig.1b-c and Extended Data Fig. 1a), the interaction with p53 was specific for the class I PITPs, indicating specificity within the family. Moreover, the small heat shock proteins (sHSPs) Hsp27 and αB-crystallin, which stabilize the p53-PIP_n complex[18], were also detected as stress-regulated components of the PITPα/β-p53 complex (Fig. 3d,g,h,j,k and Extended Data Fig. 5a,c,d). Additionally, *in vitro* binding studies with recombinant PITPα/β proteins and p53 demonstrated a high-affinity, saturable binding of class I PITPs to p53 (Fig. 3l-o). Consistent with these results, PITPβ bound p53 with 19+/-2 nM affinity as determined by microscale thermophoresis (MST) and their affinity was increased to 5+/-1 nM by adding PI (Table 1), indicating that PI regulates the class I PITP/p53 interaction. Collectively, these data show that PITPα/β form a nuclear complex with p53 in response to stress and that PI loading of PITPs enhances this interaction (Fig. 3p).

PITPα/β control the PIP_n linkage to p53 and other proteins

As PITPα/β regulate nuclear PIP_n levels and bind to p53 in the nucleus, we examined the potential role of PITPα/β in regulating the PIP_n interactions with p53, which stabilize p53[18]. The p53-PIP_n complexes[17, 18] were first analyzed by PLA, an established approach to

detect posttranslational modifications (PTMs) on proteins and molecules in close proximity *in* situ[32, 35]. Single or combined KD of PITPα/β, but not PITPNC1, reduced or largely eliminated, respectively, $p53^{mt}$-$PI4,5P_2$ and $p53^{mt}$-$PI3,4,5P_3$ complexes detected by PLA; combined KD of PITPα/β disrupted $p53^{mt}$-PIP_n complexes to a similar degree as p53 KD (Fig. 4a-c and Extended Data Fig. 6a,b). Similar results were observed in $p53^{wt}$ cells: individual or combined PITPα/β KD inhibited $p53^{wt}$-$PI4,5P_2$ and $p53^{wt}$-$PI3,4,5P_3$ complexes (Fig. 4d-f and Extended Data Fig. 6c). We next quantified the cisplatin-induced PIP_n isoforms linked to p53 by p53-IP followed by simultaneous Western blotting (WB) with antibodies (Abs) against specific PIP_n isoforms detected with fluorescently labeled secondary Abs (IP fluorescent-WB) (Fig. 4g and Extended Data Fig. 6d). KD of PITPα or PITPβ markedly reduced the PI4P, $PI4,5P_2$ and $PI3,4,5P_3$ that co-IPed with $p53^{mt}$ in response to genotoxic stress, while the combined KD largely eliminated all PIP_ns associated with $p53^{mt}$ (Fig. 4h-k). To further define the p53-PIP_n linkage, cells with $p53^{mt}$ were metabolically labeled with [^{3}H]*myo*-inositol, a standard approach to specifically label phosphoinositides and their downstream metabolites in cells[36-38]. p53 was IPed in labeled cells, and lysates were analyzed by WB after SDS-PAGE, which revealed [^{3}H]*myo*-inositol incorporated into p53 that corresponded to the cisplatin-induced $PI4,5P_2$ detected by WB (Fig. 4l,m). Similar observations were made in cells with $p53^{wt}$: single or combined PITPα/β KD also inhibited cisplatin-stimulated $p53^{wt}$-$PI4,5P_2$ complex formation (Fig. 4n,o). The findings here indicate that class I PITPα and PITPβ play a key role in the stress-responsive coupling of PIP_ns to $p53^{wt}$ and $p53^{mt}$ proteins, which are resistant to denaturation and SDS-PAGE analysis.

Consistent with the reported role of PIP_ns in stabilizing p53[18], KD of PITPα or PITPβ, but not PITPNC1, modestly reduced $p53^{mt}$ levels in cells under basal and stressed conditions, while the combined KD of PITPα and PITPβ robustly suppressed $p53^{mt}$ levels (Fig. 5a). The induction of $p53^{wt}$ by cisplatin was dramatic and was markedly inhibited by individual PITPα/β KD and abrogated by combined PITPα/β KD (Fig. 5b). Remarkably, WBs of whole cell lysates with antibodies specific for PI4P, $PI4,5P_2$ or $PI3,4,5P_3$ detected multiple protein bands, including some that were enhanced by genotoxic stress after 24 hours (Fig. 5b-f and Extended Data Fig. 6e), indicating that PIP_ns are linked to additional proteins. Individual and combined KD of PITPα/β robustly reduced the protein-coupled $PI4,5P_2$ levels and $PI4,5P_2$ bound to $p53^{mt}$ in response to stress (Fig. 5c,d). This phenotype was recapitulated using a lenti-CRISPR knock out (KO) system. MDA-MB-231 Cas9 expressing cells (MDA-MB-231^{Cas9}) were transfected with PITPβ gRNA or non-targeting gRNA to generate PITPβ KO and control KO cells, respectively. Furthermore, single targeting of PITPα/β (KD or KO), but not PITPNC1, reduced levels of multiple protein-bound PIP_ns (PI4P, $PI4,5P_2$, $PI3,4,5P_3$) and many protein bands detected by PIP_n-specific antibodies in whole cell lysates, while combined PITPα/β targeting had a more dramatic effect (Fig. 5b-f and Extended Data Fig. 6f). Combined KD of PITPα/β also reduced [^{3}H]*myo*-inositol labelling of total cellular proteins isolated by two complementary approaches, chloroform/methanol extraction followed by acetone precipitation and extraction of proteins from SDS-PAGE gels (Fig. 5g and Extended Data Fig. 6g,h). Overall, our findings point to a much broader signaling pathway whereby PITPα/β regulate PIP_n linkage to multiple cellular proteins. Moreover, the detection of PIP_n-protein

complexes by WB with PIP_n isomer specific antibodies and by metabolic labeling with [^{3}H]*myo*-inositol after denaturing/solvent extraction indicate a highly stable interaction.

PI4KIIα interacts with p53 and cooperates with PITPα/β to synthesize p53-PI4P

As PITPα/β have been reported to cooperate with PI 4-kinases (PI4Ks) to synthesize PI4P[31, 39, 40], we postulated that one or more PI4Ks acted in concert with PITPα/β to generate p53-PI4P. To investigate this possibility, each of the four human PI4Ks[41] was individually knocked down, and the effects on p53-PI4P complexes were determined by PLA. Only individual KD of PI4KIIα suppressed basal and cisplatin-stimulated p53-PI4P levels, while combined KD of PI4KIIα and PI4KIIIα reduced p53-PI4P levels to a comparable degree as PI4KIIα KD alone (Fig. 6a,b and Extended Data Fig. 6i). p53-PI4P is the substrate for PIPKIα to synthesize p53-PI4,5P_2, which stabilizes p53[18]. Consistent with its role in generating p53-PI4P, PI4KIIα KD, but not KD of other PI4Ks, inhibited cisplatin-stimulated p53 levels (Fig. 6c). Moreover, KD of PI4KIIα mimicked the effects of PIPKIα KD in suppressing p53 induction by cisplatin, and combined KD of PI4KIIα and PIPKIα was equivalent to either individual KD with regard to p53 levels (Fig. 6d). In contrast to PI4KIIα KD which reduced p53-PI4P levels, KD of PIPKIα enhanced p53-PI4P levels (Fig. 6e,f and Extended Data Fig. 6j). Functionally, PI4KIIα co-IPed with $p53^{mt}$ and $p53^{wt}$, and these interactions were enhanced by genotoxic stress (Fig. 6g). PI4KIIIα also co-IPed with $p53^{mt}$ and $p53^{wt}$, but PI4KIIIα KD did not affect p53 or p53-PI4P levels or enhance the effects of PI4KIIα KD (Fig. 6a-c). Recombinant PI4KIIα binding to p53 was saturable with 8+/-2 nM affinity (Extended Data Fig. 7a and Table 1) consistent with a specific and direct interaction. These findings indicate that PI4KIIα binds to p53 with high

affinity and is the PI 4-kinase that specifically synthesizes p53-PI4P and contributes to p53 stabilization by generating the precursor for p53-PI4,5P_2.

An emerging concept is that PITPs enhance the activity of PI4Ks ("instructive regulation") to facilitate free PI4P lipid synthesis[39, 42]. Consistent with this model, PITPα and PITPβ directly bound PI4KIIα with high affinity, and these interactions were enhanced by PI (Extended Data Fig. 7b,c and Table 1). Furthermore, KD of PI4KIIα phenocopied the effects of combined KD of PITPα/β in inhibiting protein-PIP_n complexes detected by WB with PIP_n antibodies (Extended Data Fig. 7d). Similarly, KD of PITPα or PI4KIIα in MDA-MB-231 cells with PITPβ KO further reduced the protein-PIP_n signals by WB (Fig. 6h and Extended Data Fig. 7e). PI4KIIα KD also reduced nuclear PI4,5P_2 content determined by IF (Fig. 6i and Extended Data Fig. 7f,g), indicating that PI4KIIα, like PITPα/β, plays a key functional role in generating the nuclear PIP_n pools. These data indicate that PITPα/β and PI4KIIα act in concert to initiate nuclear PIP_n signaling on p53 and other cellular proteins (Fig. 6j).

PITPα/β regulate p53-PIP_n signalosome formation and nuclear Akt activation to inhibit stress-induced apoptosis

The p53-PIP_n signalosome is regulated by cellular stress, leading to the formation of p53-PI3,4,5P_3 complexes that recruit and activate Akt in the nucleus and protect cells from stress-induced apoptosis[17]. The identification of class I PITPs as upstream regulators of p53-PIP_n complex assembly implicates these lipid transfer proteins in nuclear Akt activation. Consistent with this concept, individual KD of PITPα or PITPβ, but not PITPNC1, suppressed stress-induced nuclear Akt activation quantified by nuclear

pAkt^{S473} IF, and combined PITPα/β KD resulted in a more robust inhibition (Fig. 7a,b). Similar results were obtained with multiple human cancer cell lines expressing p53^{mt} (Fig. 7c-e and Fig. 2e). KD of p53^{mt}, PITPα or PITPβ, but not PITPNC1, moderately reduced cell viability under basal conditions and sensitized MDA-MB-231 cells to cisplatin treatment as did KO of PITPβ, while KD of PITPα in MDA-MB-231 cells with PITPβ KO or combined PITPα/β KD in parental cells further decreased cell viability (Fig. 7f-h, Extended Data Fig. 7h, and Extended Data Fig. 8a-g). The cytotoxicity of p53^{mt} KD and individual and combined PITPα/β KD was associated with a corresponding increase in caspase 3 activity (Fig. 7i and Extended Data Fig. 8e-j), indicating that PITPα/β KD triggers apoptosis and sensitizes cells to genotoxic stress. These findings underscore the regulation of nuclear Akt activation by PITPα/β, which confers resistance to genotoxic stress-induced apoptosis.

As PITPα/β exchange PI for PC, we investigated whether the PI transfer activity of these PITPs was required to regulate nuclear PIP_n pools and nuclear Akt activation. For this, we utilized the PITPα/β^{T59D} mutant that specifically disrupts PI binding[43-45]. Ectopically expressed HA-tagged PITPα/β^{wt} interacted with p53^{wt} and mutant p53^{R175H}, while the corresponding PITPα/β^{T59D} mutants exhibited impaired interaction with p53 (Fig. 8a and Extended Data Fig. 8k-m). Moreover, the reduction in the stress-induced nuclear PI4,5P_2 pool and nuclear pAkt^{S473} levels by combined PITPα and PITPβ KD using distinct siRNAs targeting their 3'-UTR was rescued by expression of PITPα^{wt}, but not mutant PITPα^{T59D} (Fig. 8b-e). Notably, the nuclear PI4,5P_2 and pAkt^{S473} levels correlated with the content of

re-expressed PITPα^{wt}, but not mutant PITPα^{T59D} (Fig. 8f-i), indicating that these phenotypes are dose-dependent.

The cytotoxicity and sensitization to cisplatin-induced apoptosis by combined PITPα/β KD using the 3'-UTR targeting siRNAs were partly rescued by re-expressing PITPα^{wt} but not the PITPα/β^{T59D} mutant (Fig. 8j,k and Extended Data Fig. 8n). Combined PITPα/β KD also inhibited EGF-stimulated cell invasion and these effects were partly restored by re-expressing PITPα^{wt} but not the PITPα^{T59D} mutant (Fig. 8l,m). These results demonstrate that the PI transfer activity of class I PITPs regulates their interaction with p53 and related nuclear Akt activation. The data also suggest a broader role for PITPα/β in regulating PIP_n linkage to additional proteins beyond p53 that may contribute to cell growth, invasion and protection against genotoxic stress (Fig. 8n).

Discussion

Here we reveal an unexpected role for class I PITPα/β in generating nuclear PIP_n pools that initiate PIP_n signaling. Although the existence of nuclear PIP_ns and their role in the cell cycle[46], oxidative stress[16, 47-52] and the DNA damage response[17, 53-55] is supported by growing evidence[16], the molecular origin of nuclear PIP_ns in regions devoid of membranes has been enigmatic[56]. PITPs have a well-established role in transporting PI from the endoplasmic reticulum to membranes to enable membrane-localized PIP_n signaling via PIP kinases, phosphatases, and phospholipase-C[25-28, 31, 57]. The findings presented here demonstrate that PITPs accumulate in the non-membranous nucleoplasm in response to diverse cellular stressors to regulate the membrane-free nuclear PIP_n pools. As such, these data expand the roles of the PITP lipid transport activities that were thought to act

largely in the cytosol and establish their mechanistic roles in generating nuclear PIP_n pools.

In addition, PITPα/β, but not other PITP family members, bind directly to $p53^{wt}$ and $p53^{mt}$ and these interactions are stimulated by cell stress. This complex also includes the small heat shock proteins (Hsp27 and αB-crystallin), which stabilize p53[18]. PITPα/β binding to p53 is necessary for the linkage of PIP_ns with p53 (p53-PIP_n signalosome). Once the p53-PIP_n linkage is formed it is stable and detected by PIP_n isomer antibodies and acted on by multiple PIP kinases and phosphatases, indicating that the myo-inositol head group is accessible and can be utilized as a substrate for these enzymes[17, 18, 32]. This p53-PIP_n pathway culminates in the formation of p53-PI3,4,5P_3 complexes that in turn, recruit and activate Akt in the nucleus, conferring resistance to stress-induced apoptosis[17]. These PITPα/β activities require PI binding, underscoring the critical functional role of lipid transport in nuclear PIP_n signaling. Indeed, the ability of wild-type PITPα, but not the PI binding-defective mutant, to rescue the phenotype of combined PITPα/β KD suggests a functional redundancy of PITPα and PITPβ for nuclear phosphoinositide signaling. This is consistent with previous reports that either PITPα or PITPβ is sufficient to rescue the phenotype of double PITPα/β knockout in a PI-binding dependent manner[43, 58]. PITPα/β interact with the PI 4-kinase PI4KIIα, and both also bind p53 and are required to generate the p53-PI4P complex, pointing to a functional collaboration between PITPα/β and PI4KIIα in initiating nuclear PIP_n signaling that is highly reminiscent of their roles in generating PI4P in the membrane-localized pathway[39, 40].

Remarkably, PITPα/β and PI4KIIα regulate the coupling of PIP_ns to a suite of cellular proteins that are detected by WB with PIP_n isomers antibodies and by metabolic labelling cells with [^{3}H]*myo*-inositol. These data indicate that the nuclear IF staining of PIP_ns is a composite of PIP_n-linked proteins. Furthermore, our observation that the p53-PIP_n and protein-PIP_n linkages can be detected by metabolic labelling with [^{3}H]*myo*-inositol and are resistant to denaturation and solvent extraction indicates a tight coupling consistent with a putative posttranslational modification. Indeed, our data indicate PIP_n second messengers are linked to p53 and other proteins by the combined activities of PITPα/β and PI4KIIα. The resulting p53-PI4P is acted on by PIP kinases and phosphatases such that the PI3,4,5P_3 linked to p53 acts as a messenger to recruit PDK1, mTORC2, and Akt, culminating in nuclear Akt activation and stress-resistance. These findings suggest a "third messenger" pathway with p53 as the founding member whereby PIP_n second messengers are linked to cellular proteins in membrane-free regions and modified by PIP kinases/phosphatases to regulate their function (Fig. 8n). The assembly of distinct PIP_n isomer-protein complexes with unique binding partners has the potential to enable exquisite spatial and temporal regulation of signaling cascades anchored on cellular proteins instead of membranes. Although the focus here is on the nuclear pathway, there is nothing *per se* that limits PIP_n-linked proteins to the nucleus and p53-PI4P detected by PLA is both nuclear and cytosolic. Given the critical role of class I PITPs in initiating nuclear phosphoinositide signaling, which attenuates cellular stress and apoptosis, these findings also point to these PITPs and PI4KIIα as potential therapeutic targets in a variety of diseases including cancer.

ACKNOWLEDGMENTS

We thank Dr. Adrea Galmozzi for discussions and comments, and Lance Rodenkirch for technical support. N.D.C. is supported by a National Institutes of Health T32 Training Grant 5T32ES007015-43 to the Molecular and Environmental Toxicology graduate training program at UW-Madison. M.C. is supported by grant D2301007 from the Shenzhen Medical Research Fund. This work was supported in part by a National Institutes of Health grant R35GM134955 (R.A.A.), Department of Defense Breast Cancer Research Program grants W81XWH-17-1-0258 (R.A.A.), W81XWH-17-1-0259 (V.L.C.), W81XWH-21-1-0129 (V.L.C.), HT9425-23-1-0553 (V.L.C.), and HT9425-23-1-0554 (R.A.A.), and a grant from the Breast Cancer Research Foundation (V.L.C.).

AUTHOR CONTRIBUTIONS

M.C., N.D.C, V.L.C., and R.A.A. designed the experiments. N.D.C., M.C., T.W., P.A., and T.J.W. performed the experiments. N.D.C., M.C., V.L.C., and R.A.A. wrote the manuscript.

DECLARATION OF INTERESTS

Authors declare that they have no competing interests.

METHODS

Cell culture and constructs

A549, BT-549, Cal33, HCT116, HS578T, MDA-MB-231, SUM159, SUM1315, HEK293FT, and MCF-10A cells were purchased from ATCC. MCF10A cells were cultured in DMEM/F12 (#11330-032, Invitrogen) supplemented with 10% fetal bovine serum (#SH30910.03, Hyclone), 1% penicillin/streptomycin (#15140-122, Gibco), 20 ng/mL EGF

(#CC-4107, Lonza), 0.5 mg/mL Hydrocortisone (#H4001, Sigma), 100 ng/mL Cholera toxin (#C-8052, Sigma), and 10 μg/mL Insulin (#I-1882, Sigma). The other cells were maintained in DMEM (#10-013-CV, Corning) supplemented with 10% fetal bovine serum (#SH30910.03, Hyclone) and 1% penicillin/streptomycin (#15140-122, Gibco). The cell lines used in this study were routinely tested for mycoplasma contamination using MycoAlert Mycoplasma Detection Kit (#LT07-318, Lonza), and mycoplasma-negative cells were used. None of the cell lines used in this study are listed in the database of commonly misidentified cell lines maintained by ICLAC. The p53 Flag-tagged wild-type and R175H mutant constructs used for this work were described previously[18]. The HA-tagged wild-type PITPα/β constructs and PI-binding deficient mutants T59D[43] were purchased from Genscript. Plasmids were transfected into mammalian cells using Lipofectamine™3000, (#L3000015, Thermo Fisher Scientific) according to the manufacturer's instructions. Typically, 2-5 μg of DNA and 6-10 μl of lipid were used for transfecting cells in 6-well plates. Cells with at least 80% transfection efficiency were used for further analysis.

Antibodies and reagents

Monoclonal antibodies against p53 (clone DO-1, #SC-126, Santa Cruz Biotechnology), p53 (clone 7F5, #2527, Cell Signaling), pAkt^{S473} (clone 193H12, #4058, Cell Signaling), HA-tag (clone C29F4, #3724, Cell Signaling), Flag-tag (clone D6W5B, #14793, Cell Signaling), GAPDH (clone 0411, #sc-47724, Santa Cruz Biotechnology), Lamin B2 (clone D8P3U, #12255, Cell Signaling), EGFR (clone D6B6, #2085, Cell Signaling), HSP27 (clone D6W5V, #95357, Cell Signaling), and polyclonal antibodies against PITPα

(#16613-1-AP, ThermoFisher), PITPβ (#ab127563, abcam), PITPNC1 (IF, #ab222078, abcam), PITPNC1 (WB, #NBP2-19842, Novus), PITPNM1 (#26983-1-AP, Proteintech), PITPNM2 (#PA5-48616, Invitrogen), PI4KIIα (#NBP2-44158, Novus), PI4KIIIα (#4902S, CST), PI4KIIβ (#PA5-82133, Thermo), PI4KIIIβ (#ab134756, abcam), and αB-Crystallin (#ADI-SPA-223-F, Enzo) were used in this study. For conventional immunostaining and PLA analysis of phosphoinositides, anti-PI4P (#Z-P004), PI4,5P_2 (#Z-P045) and PI3,4,5P_3 (#Z-P345) antibodies were purchased from Echelon Biosciences. For immunoblotting analyses, antibodies were diluted at a 1:1000 ratio except for p53 (clone DO-1, 1:5000) and GAPDH (clone 0411, 1:5000). For immunoprecipitation, antibody-conjugated agarose was purchased from Santa Cruz Biotechnology, including agarose-conjugated antibodies against p53 (#sc-126AC), PITPα/β (#sc-398050AC), HA-tag (#sc-7392AC), and Flag-tag (#sc-166355AC). For immunostaining analyses and proximity ligation assay (PLA), antibodies were diluted at a 1:100 ratio. Nuclear envelope marker (Alexa Fluor®488 Lamin A/C, clone 4C11, #8617, Cell Signaling, 1:200) was used to examine subnuclear regions. For the knockdown (KD) experiments, the ON-TARGETplus siRNA SMARTpool with 4 siRNAs in combination against human p53 (#L-003329-00), PITPα (#L-018010-00), PITPβ (#L-006459-01), and PITPNC1 (#L-012476-02) were purchased from Dharmacon. Non-targeting siRNA (#D-001810-01, Dharmacon) was used as a control. For the KD and rescue experiments, pooled-siRNAs targeting the 3'UTR of PITPα (sense 5'-AGGCAACUUUCGAUUCCUUACUGUA-3' and antisense 5'-UACAGUAAGGAAUCGAAAGUUGCCU-3'; sense 5'-CCGUCUCUCUCCAUUGUGUUCCGAU-3' and antisense 5'-AUCGGAACACAAUGGAGAGAGACGG-3') and pooled-siRNAs targeting the 3'UTR of

PITPβ (sense 5'- GAGUGAACAACAAUCUGACCAGUAU-3' and antisense 5'-AUACUGGUCAGAUUGUUGUUCACUC-3'; sense 5'- CUACAAAGCUGAUGAAGAC-3' and antisense 5'-GUCUUCAUCAGCUUUGUAG-3') were purchased from Thermo Fisher Scientific. The siRNAs were delivered to cells by RNAiMAX reagent (#13778150, Thermo Fisher Scientific), and KD efficiency was determined by immunoblotting. KD efficiency greater than 80% was required to observe phenotypic changes in the study. Cisplatin, (#NC1706394, Fisher Scientific), etoposide (#S1225, Sellekchem), Erastin (#S7242, Selleckchem), tert-Butylhydroquinone (tBHQ, #SPCM-T1540-06, Spectrum), and hydroxyurea (HU, #1332000, Millipore Sigma) were used as cellular stressors.

Immunoprecipitation and immunoblotting

Cells were removed from the medium after the indicated treatment, washed three times with ice-cold PBS, and lysed in an ice-cold RIPA lysis buffer system (#sc-24948, Santa Cruz Biotechnology) with 1 mM Na_3VO_4, 5 mM NaF, and 1x protease inhibitor cocktail (#11836153001, Roche). The cell lysates were then sonicated at 15% amplitude for 15 s. After sonication, the cell lysates were incubated at 4°C with continuous rotation for 1 h and subsequently centrifuged at maximum speed for 10 min to collect the supernatant. The protein concentration in the supernatant was measured by the Bradford protein assay (#5000201, BIO-RAD) according to the manufacturer's instructions. Equal amounts of protein were used for further analysis. All antibodies were diluted at a 1:1000 ratio for immunoblotting unless otherwise indicated. For immunoprecipitation, 0.5-1 mg of protein was incubated with 20 μl of antibody-conjugated agarose (Santa Cruz Biotechnology) at 4°C for 24 h. After washing three times with PBST (PBS with 0.1% Tween 20), the protein

complex was eluted with SDS sample buffer and boiled at 95°C for 10 min. For immunoblotting, 5-20 μg of protein were loaded. For immunoblotting of immunoprecipitated complexes, horseradish peroxidase (HRP)-conjugated antibodies were used to avoid non-specific detection of immunoglobulin in the immunoprecipitated samples. HRP-conjugated p53 (#sc-126HRP), PITPα (#sc-13569HRP), PITPβ (#sc-390500HRP) antibodies were purchased from Santa Cruz Biotechnology. Immunoblots were developed by Odyssey Imaging System (LI-COR Biosciences) and the intensity of protein bands was quantified using ImageJ. The unsaturated exposure of immunoblot images was used for quantification with the appropriate loading controls as standards. Statistical data analysis was performed with Microsoft Excel, using data from at least three independent experiments.

Fluorescent IP-WB

Cells were lysed in a RIPA lysis buffer system after the indicated treatment and quantified for protein concentration as described above. For endogenous p53 or FLAG-tagged p53 immunoprecipitation, 0.5-1 mg of cell lysates were incubated with 20 μl anti-p53 (#sc-126 AC, Santa Cruz Biotechnology) or anti-FLAG (#sc-166355AC, Santa Cruz Biotechnology) mouse monoclonal IgG antibody-conjugated agarose at 4°C for 24 h. Normal immunoglobulin (IgG)-conjugated agarose was used as a negative control (#sc-2343, Santa Cruz Biotechnology). After washing three times with PBST, the protein complex was eluted with SDS sample buffer. The sample was then boiled at 95°C for 10 min. For immunoblotting, 5-20 μg of protein were loaded. The protein complexes associated with p53 were resolved by SDS-PAGE and transferred onto a PVDF membrane (#IPVH00010,

MilliporeSigma). The membrane was blocked with 1% BSA in TBS for 1 h at room temperature. For double fluorescent IP-WB detecting p53-PI4P/PI4,5P_2/PI3,4,5P_3 complexes, anti-p53 rabbit monoclonal IgG antibody (clone 7F5, #2527, Cell Signaling) at 1:2000 dilution and anti-PI4P mouse monoclonal IgM antibody (#Z-P004, Echelon Biosciences), PI4,5P_2 mouse monoclonal IgM antibody (#Z-P045, Echelon Biosciences), or PI3,4,5P_3 mouse monoclonal IgM antibody (#Z-P345, Echelon Biosciences) at 1:1000 dilution were mixed together in blocking buffer with 0.02 % Sodium Azide and incubated with the membrane at 4°C overnight. The next day, the membrane was washed three times with TBST for 10 min each time. For the secondary antibody incubation, goat anti-rabbit IgG antibody conjugated with IRDye 800CW fluorophore (#926-32211, LI-COR) detectable on the 800 nm wavelength channel of the Odyssey Fc Imaging System (LI-COR Biosciences) and goat anti-mouse IgM antibody conjugated with IRDye 680RD fluorophore (#926-68180, LI-COR) detectable on the 700 nm wavelength channel at 1:10000 dilution were mixed in blocking buffer with 0.01 % SDS and 0.1% Tween 20 and incubated with the membrane at room temperature for 2 h. The membrane was then washed three times with TBST for 10 min each time. The images were subsequently acquired simultaneously using the 700 and 800 nm wavelength channels on the Odyssey Fc Imaging System (LI-COR Biosciences). The p53-associated PI4P/PI4,5P_2/PI3,4,5P_3 complex was visualized by overlapping the 700 and 800 nm channels. Statistical data analysis was performed with Microsoft Excel, using data from at least three independent experiments.

***In vitro* binding assay**

The recombinant proteins p53 (#81091, Active Motif), PITPα (#ab101666, Abcam), PITPβ (#LS-C794864, LSBio), and PI4KIIα (lab made) were used for *In Vitro* binding assays. The binding assay was performed in PBS by incubating a constant amount of p53 with an increasing amount of PITPα/β or PI4KIIα in the presence of 20 µl anti-p53 antibody-conjugated agarose (#sc-126AC, Santa Cruz). After incubating overnight at 4°C, unbound proteins were removed by washing three times with PBST, and the protein complex was analyzed by immunoblotting.

Immunofluorescence (IF) and Confocal Microscopy

For immunofluorescence studies, cells were grown on coverslips coated with 0.2 % gelatin (#G9391, MilliporeSigma). Cells were fixed with 4% paraformaldehyde (PFA) (#sc-281692, Santa Cruz Biotechnology) for 20 min at room temperature followed by washing three times with PBS. Next, the cells were permeabilized with 0.3% Triton-X100 for 30 min to thoroughly permeate the nuclear envelope and rewashed three times with PBS. The cells were then blocked with 1% BSA in PBS for one hour at room temperature. After blocking, cells were incubated with primary antibodies overnight at 4°C. The cells were then washed three times with PBS and incubated with fluorescent-conjugated secondary antibodies (Molecular Probes) for 1 hour at room temperature. After secondary antibody incubation, the cells were washed three times. Then the coverslips were taken out from the dishes, air-dried for 10 min at room temperature and mounted in Prolong™ Glass Antifade Mountant with NucBlue™ Stain (#P36985, Thermo Fisher Scientific). The images were taken by Leica SP8 3xSTED Super-Resolution Microscope, which is both a point scanning confocal and 3xSTED super-resolution microscope. The Leica SP8

3xSTED microscope was controlled by LASX software (Leica Microsystems). All images were acquired using the 100X objective lens (N.A. 1.4 oil). The z-stack images were taken with each frame over a 0.2 μm thickness. For quantification, the mean fluorescent intensity of channels in each cell was measured by LASX. GraphPad Prism Version 9.4.1 generated quantitative graphs. The images were processed using ImageJ. The correlation of double staining channels was quantified by GraphPad Prism using Pearson's correlation coefficient (Pearson's r), ranging between 1 and −1. A value of 1 represents perfect correlation, 0 means no correlation, and -1 means perfect negative correlation[59]. Pearson's r greater than 0.7 suggests a strong correlation[60].

Proximity Ligation Assay (PLA)

PLA was utilized to detect *in situ* protein-protein/PIP_n interaction as previously described [17, 18, 32]. After fixation and permeabilization, cells were blocked before incubation with primary antibodies as in routine IF staining. The cells were then processed for PLA (#DUO92101, MilliporeSigma) according to the manufacturer's instruction and previous publications [17, 18, 32]. Post-PLA slides were further processed for immunofluorescent staining against the nuclear membrane marker (Lamin A/C, #8617, Cell Signaling). After washing three times with PBST, the slides were mounted with Prolong™ Glass Antifade Mountant with NucBlue™ Stain (#P36985, Thermo Fisher Scientific). The Leica SP8 confocal microscope detected PLA signals as discrete punctate foci and provided the intracellular localization of the complex. ImageJ was used to quantify the nuclear PLA foci.

Crystal Violet Cell Viability assay

In 96-well plates, 5×10^4 cells/well of MDA-MB-231, MDA-MB-231^{Cas9}, BT549, SUM159, or SUM1315 cells were transfected with control siRNAs or siRNAs targeting p53, PITPα, PITPβ, PITPNC1, or the combination of PITPα and PITPβ as indicated for 48 h. For the KD rescue experiments, MDA-MB-231 cells were transfected with control siRNAs or siRNAs targeting 3'UTR of PITPα and PITPβ for 24 h. Next, the cells were transfected with either HA-tagged wild-type PITPα or its PI-binding deficient T59D mutant PITPα for another 24 h. The cells were then treated with the control vehicle or 30 μM cisplatin for 24 h, and the cells were subsequently fixed with 4% PFA and stained with 0.2% Crystal Violet. After washing the cells 3 times with PBS, the plates were air-dried at room temperature and imaged using EVOS M5000 Imaging System (ThermoFisher Scientific). After imaging, the dye was extracted from the cells with 10% acetic acid and quantified by measuring the absorbance at 570 nm using a Synergy HTX Multi-Mode Microplate reader.

Caspase 3 Activity Assay

In 6-well plates, 1×10^6 cells/well of MDA-MB-231, BT549, SUM159, or SUM1315 were transfected with control siRNAs or siRNAs targeting p53, PITPα, PITPβ, PITPNC1, or the combination of PITPα and PITPβ as indicated for 48 h. For the KD rescue experiments, MDA-MB-231 cells were transfected with control siRNAs or siRNAs targeting 3'UTR of PITPα and PITPβ for 24 h. Then the cells were transfected with either HA-tagged wild-type PITPα or its PI-binding deficient T59D mutant PITPα for another 24 h, followed by treatment with control vehicle or 30 μM cisplatin for 24 h. Next, the cells were lysed and processed for Caspase 3 activity assay by following the manufacturer's instructions (#E-

13183, Thermo Fisher Scientific). At the end of the assay, the fluorescence was read at excitation/emission 342/441 nm using a Synergy HTX Multi-Mode Microplate reader.

Transwell Invasion Assay

The bottom polycarbonate filter surface of a 6.5 mm diameter insert with 8 μm pores in a 24-well plate (#3422, Corning) was coated with 10 μg/ml of Laminin (#CC095, MilliporeSigma) diluted in PBS for 3 h at 37ºC. MDA-MB-231 cells were transiently transfected with control siRNAs or siRNAs targeting the 3'UTR of both PITPα and PITPβ for 24 h. Then the cells were transfected with either HA-tagged wild-type PITPα or its PI-binding deficient T59D mutant PITPα. After 24 h, cells were serum starved for an additional 24 h. Next, $5x10^4$ transfected cells were suspended in 200 μl serum-free medium containing 0.5% BSA and then were plated in the upper insert chamber in 500 μl serum-free medium with 0.5% BSA. 10 ng/ml EGF was added to the lower chamber. Cells were allowed to invade for 16 h at 37°C. Cells on the bottom of the filter were then fixed with 4% PFA and stained with 0.2% Crystal Violet. The stained cells were imaged using EVOS M5000 Imaging System (ThermoFisher Scientific). At the end of the assay, the dye was extracted by 10% acetic acid from the cells and quantified by measuring the optical density at 570 nm using a Synergy HTX Multi-Mode Microplate reader.

Microscale Thermophoresis (MST) Assay

The microscale thermophoresis (MST) assay was used to calculate the binding affinities of purified recombinant proteins (p53 (#81091, Active Motif), PITPα (#ab101666, Abcam), PITPβ (#LS-C794864, LSBio), PI4KIIα (lab made)) and other contributing factors *in vitro*

as previously described[61]. The target protein was fluorescently labeled using a Monolith Protein Labeling kit (RED-NHS 2nd Generation MO-L011, Nano Temper) following the manufacturer's instruction. Then, sequential titration of unlabeled ligand proteins or PI (#840042P, Avanti), was made in a Tris-based MST buffer containing 50 mM Tris-HCl, pH 8.0, 50 mM NaCl, 80 mM KCl and 0.05% Tween 20 and mixed with an equal volume of fluorescently labelled target protein prepared at 10 nM concentration in the same MST buffer, making the final target protein at a constant concentration of 5 nM and the ligand protein or lipid as the gradient. For PI cofactor analysis, target proteins were mixed with 1 μM PI prior to ligand proteins and PI concentration remained constant across the gradient of ligand protein. The target–ligand mixtures were loaded into Monolith NT.115 series capillaries (MO-K022, Nano Temper), and the MST traces were measured using Monolith NT.115 pico. The binding affinity was autogenerated using MO Control v.1.6 software.

[^{3}H]*myo*-inositol Metabolic Labeling

Cells were split and cultured in low serum Opti-MEM (#31985070, Thermo) supplemented with 10% dialyzed FBS with a 10,000 mw cut-off (#F0392, Sigma) and 1% Pen/strep (#15140-122, Gibco). In 10 cm dishes, 0.5×10^6 MDA-MB-231 cells were seeded to achieve ~5% confluency the following day. 24 h after plating, cells were treated with either 1.322 μM (25 μCi/mL) of [^{3}H]*myo*-inositol (#NET1156005MC, PerkinElmer) or unlabeled *myo*-inositol (#J60828.22, Thermo) and allowed to uptake the metabolic label for 48 h. For KD experiments, PITPα/β siRNAs were added and recovered as normal and fresh [^{3}H]*myo*-inositol supplemented media was used to replace the transfection media. 24 h

after siRNA transfection (72 h after original plating), cells were treated with control vehicle or 30 μM cisplatin for another 24 h. Cells were then lysed and p53 was immunoprecipitated for IP:p53 samples before performing SDS-PAGE or $CHCl_3$/MeOH extraction as indicated. SDS-PAGE samples were excised from the gel and dissolved in 30% H_2O_2 before liquid scintillation counting (LSC). Dissolved gel samples or resuspended protein samples were added to LSC vials with LSC cocktail (#6013319, PerkinElmer) before being processed by PerkinElmer Tri-Carb 4910 TR liquid scintillation analyzer. Analysis and DPM calculation were automated using QuantaSmart software.

Lenti-CRISPR Gene Editing

CRISPR-Cas9 genome-editing was used to knockout the gene encoding PITPβ in MDA-MB-231 cells. First a Cas9 expressing stable cell line was generated by transducing cells with viral particles (#LVCAS9BST, Sigma Aldrich) at the multiplicity of infection (MOI) of 0.5. Transduction was performed in complete media containing 8*μ*g/mL polybrene. After 24 h incubation, Cas9-expressing cells were selected with 10*μ*g/mL blasticidin (#DSB12150; Dot Scientific) for 1 week and expression was confirmed. To generate PITPβ KO cells, viral particles containing the guide RNA sequence for PITPβ (5'-CAATCATCCTCACGAATGC-3') and negative control (5'-CGCGATAGCGCGAATATATT-3') were purchased from Sigma Aldrich. Sequences were cloned into LV21 lentiviral vectors (Sigma Aldrich). Cas9-expressing cells were then transduced with viral particles at a MOI of 0.5 and incubated for 24 h. Transduction was performed in the presence of 8*μ*g/mL polybrene in complete media. Media was removed 24 h after viral transduction and 1500 *μ*g/mL geneticin (#10131035; Sigma Aldrich) was

added for selection. After 1 week of selection in antibiotics, single cells were isolated in the 96-well tissue culture dish by BD FACS AriaII. Cells were expanded and positive colonies were selected by immunoblotting.

Statistics and Reproducibility

Two-tailed unpaired *t*-tests were used for pair-wise significance unless otherwise indicated. We note that no power calculations were used. Sample sizes were determined based on previously published experiments where significant differences were observed[17, 18]. Each experiment was repeated at least three times independently, and the number of repeats is defined in each figure legend. We used at least three independent experiments or biologically independent samples for statistical analysis.

Resource and Data Availability

All data supporting the findings of this study are available from the corresponding authors on reasonable request.

References

1. Hammond, G.R.V. & Burke, J.E. Novel roles of phosphoinositides in signaling, lipid transport, and disease. *Curr Opin Cell Biol* **63**, 57-67 (2020).
2. Fruman, D.A. *et al.* The PI3K Pathway in Human Disease. *Cell* **170**, 605-635 (2017).
3. Hoxhaj, G. & Manning, B.D. The PI3K-AKT network at the interface of oncogenic signalling and cancer metabolism. *Nat Rev Cancer* **20**, 74-88 (2020).
4. Manning, B.D. & Toker, A. AKT/PKB Signaling: Navigating the Network. *Cell* **169**, 381-405 (2017).
5. Burke, J.E., Triscott, J., Emerling, B.M. & Hammond, G.R.V. Beyond PI3Ks: targeting phosphoinositide kinases in disease. *Nat Rev Drug Discov*, 1-30 (2022).
6. Currie, R.A. *et al.* Role of phosphatidylinositol 3,4,5-trisphosphate in regulating the activity and localization of 3-phosphoinositide-dependent protein kinase-1. *Biochem J* **337 (Pt 3)**, 575-583 (1999).
7. Liu, P. *et al.* PtdIns(3,4,5)P3-Dependent Activation of the mTORC2 Kinase Complex. *Cancer Discov* **5**, 1194-1209 (2015).
8. Calleja, V. *et al.* Intramolecular and intermolecular interactions of protein kinase B define its activation in vivo. *PLoS Biol* **5**, e95 (2007).
9. Altomare, D.A. & Testa, J.R. Perturbations of the AKT signaling pathway in human cancer. *Oncogene* **24**, 7455-7464 (2005).
10. Kondapaka, S.B., Singh, S.S., Dasmahapatra, G.P., Sausville, E.A. & Roy, K.K. Perifosine, a novel alkylphospholipid, inhibits protein kinase B activation. *Mol Cancer Ther* **2**, 1093-1103 (2003).
11. Kikani, C.K. *et al.* Proliferative and antiapoptotic signaling stimulated by nuclear-localized PDK1 results in oncogenesis. *Sci Signal* **5**, ra80 (2012).
12. Shiraishi, I. *et al.* Nuclear targeting of Akt enhances kinase activity and survival of cardiomyocytes. *Circ Res* **94**, 884-891 (2004).
13. Fu, W. & Hall, M.N. Regulation of mTORC2 Signaling. *Genes (Basel)* **11** (2020).
14. Martelli, A.M. *et al.* The emerging multiple roles of nuclear Akt. *Biochim Biophys Acta* **1823**, 2168-2178 (2012).
15. Liu, L. *et al.* DNA-PK promotes activation of the survival kinase AKT in response to DNA damage through an mTORC2-ECT2 pathway. *Sci Signal* **15**, eabh2290 (2022).
16. Chen, M. *et al.* The nuclear phosphoinositide response to stress. *Cell Cycle* **19**, 268-289 (2020).
17. Chen, M. *et al.* A p53-phosphoinositide signalosome regulates nuclear AKT activation. *Nat Cell Biol* **24**, 1099-1113 (2022).
18. Choi, S., Chen, M., Cryns, V.L. & Anderson, R.A. A nuclear phosphoinositide kinase complex regulates p53. *Nat Cell Biol* **21**, 462-475 (2019).
19. Muller, P.A. & Vousden, K.H. p53 mutations in cancer. *Nat Cell Biol* **15**, 2-8 (2013).
20. Hassin, O. & Oren, M. Drugging p53 in cancer: one protein, many targets. *Nat Rev Drug Discov* **22**, 127-144 (2023).
21. Emerling, B.M. *et al.* Depletion of a putatively druggable class of phosphatidylinositol kinases inhibits growth of p53-null tumors. *Cell* **155**, 844-857 (2013).

22. Cocco, L. *et al.* Synthesis of polyphosphoinositides in nuclei of Friend cells. Evidence for polyphosphoinositide metabolism inside the nucleus which changes with cell differentiation. *Biochem J* **248**, 765-770 (1987).
23. Boronenkov, I.V., Loijens, J.C., Umeda, M. & Anderson, R.A. Phosphoinositide signaling pathways in nuclei are associated with nuclear speckles containing pre-mRNA processing factors. *Mol Biol Cell* **9**, 3547-3560 (1998).
24. Blind, R.D. *et al.* The signaling phospholipid PIP3 creates a new interaction surface on the nuclear receptor SF-1. *Proc Natl Acad Sci U S A* **111**, 15054-15059 (2014).
25. Hunt, A.N., Clark, G.T., Attard, G.S. & Postle, A.D. Highly saturated endonuclear phosphatidylcholine is synthesized in situ and colocated with CDP-choline pathway enzymes. *J Biol Chem* **276**, 8492-8499 (2001).
26. Wang, Y., Sweitzer, T.D., Weinhold, P.A. & Kent, C. Nuclear localization of soluble CTP:phosphocholine cytidylyltransferase. *J Biol Chem* **268**, 5899-5904 (1993).
27. Tribble, E.K. *et al.* Quantitative profiling of the endonuclear glycerophospholipidome of murine embryonic fibroblasts. *J Lipid Res* **57**, 1492-1506 (2016).
28. Blunsom, N.J. & Cockcroft, S. Phosphatidylinositol synthesis at the endoplasmic reticulum. *Biochim Biophys Acta Mol Cell Biol Lipids* **1865**, 158471 (2020).
29. Bahmanyar, S. Spatial regulation of phospholipid synthesis within the nuclear envelope domain of the endoplasmic reticulum. *Nucleus-Phila* **6**, 102-106 (2015).
30. Huang, Y. *et al.* Global tumor protein p53/p63 interactome: making a case for cisplatin chemoresistance. *Cell Cycle* **11**, 2367-2379 (2012).
31. Ashlin, T.G., Blunsom, N.J. & Cockcroft, S. Courier service for phosphatidylinositol: PITPs deliver on demand. *Biochim Biophys Acta Mol Cell Biol Lipids* **1866**, 158985 (2021).
32. Chen, M., Horn, H.T., Wen, T., Cryns, V.L. & Anderson, R.A. Assessing In Situ Phosphoinositide-Protein Interactions Through Fluorescence Proximity Ligation Assay in Cultured Cells. *Methods Mol Biol* **2251**, 133-142 (2021).
33. Kalasova, I. *et al.* Tools for visualization of phosphoinositides in the cell nucleus. *Histochem Cell Biol* **145**, 485-496 (2016).
34. Balla, T. Phosphoinositides: tiny lipids with giant impact on cell regulation. *Physiol Rev* **93**, 1019-1137 (2013).
35. Oliveira, F.M.S. *et al.* Detection of post-translational modifications using solid-phase proximity ligation assay. *N Biotechnol* **45**, 51-59 (2018).
36. Wilson, M.S.C. & Saiardi, A. Importance of Radioactive Labelling to Elucidate Inositol Polyphosphate Signalling. *Top Curr Chem (Cham)* **375**, 14 (2017).
37. Hale, A.T., Clarke, B.P. & York, J.D. Metabolic Labeling of Inositol Phosphates and Phosphatidylinositols in Yeast and Mammalian Cells. *Methods Mol Biol* **2091**, 83-92 (2020).
38. Steinfeld, N., Giridharan, S.S.P., Kauffman, E.J. & Weisman, L.S. Simultaneous Detection of Phosphoinositide Lipids by Radioactive Metabolic Labeling. *Methods Mol Biol* **2251**, 1-17 (2021).
39. Lete, M.G., Tripathi, A., Chandran, V., Bankaitis, V.A. & McDermott, M.I. Lipid transfer proteins and instructive regulation of lipid kinase activities: Implications for inositol lipid signaling and disease. *Adv Biol Regul* **78**, 100740 (2020).

40. Grabon, A., Bankaitis, V.A. & McDermott, M.I. The interface between phosphatidylinositol transfer protein function and phosphoinositide signaling in higher eukaryotes. *J Lipid Res* **60**, 242-268 (2019).
41. Boura, E. & Nencka, R. Phosphatidylinositol 4-kinases: Function, structure, and inhibition. *Exp Cell Res* **337**, 136-145 (2015).
42. Grabon, A., Khan, D. & Bankaitis, V.A. Phosphatidylinositol transfer proteins and instructive regulation of lipid kinase biology. *Biochim Biophys Acta* **1851**, 724-735 (2015).
43. Xie, Z., Hur, S.K., Zhao, L., Abrams, C.S. & Bankaitis, V.A. A Golgi Lipid Signaling Pathway Controls Apical Golgi Distribution and Cell Polarity during Neurogenesis. *Dev Cell* **44**, 725-740 e724 (2018).
44. Tilley, S.J. *et al.* Structure-function analysis of human [corrected] phosphatidylinositol transfer protein alpha bound to phosphatidylinositol. *Structure* **12**, 317-326 (2004).
45. Alb, J.G., Jr., Gedvilaite, A., Cartee, R.T., Skinner, H.B. & Bankaitis, V.A. Mutant rat phosphatidylinositol/phosphatidylcholine transfer proteins specifically defective in phosphatidylinositol transfer: implications for the regulation of phospholipid transfer activity. *Proc Natl Acad Sci U S A* **92**, 8826-8830 (1995).
46. Stallings, J.D., Tall, E.G., Pentyala, S. & Rebecchi, M.J. Nuclear translocation of phospholipase C-delta1 is linked to the cell cycle and nuclear phosphatidylinositol 4,5-bisphosphate. *J Biol Chem* **280**, 22060-22069 (2005).
47. Jones, D.R. *et al.* Nuclear PtdIns5P as a transducer of stress signaling: an in vivo role for PIP4Kbeta. *Mol Cell* **23**, 685-695 (2006).
48. Bua, D.J., Martin, G.M., Binda, O. & Gozani, O. Nuclear phosphatidylinositol-5-phosphate regulates ING2 stability at discrete chromatin targets in response to DNA damage. *Sci Rep* **3**, 2137 (2013).
49. Yokogawa, T. *et al.* Evidence that 3 '-phosphorylated polyphosphoinositides are generated at the nuclear surface: use of immunostaining technique with monoclonal antibodies specific for PI 3,4-P-2. *Febs Lett* **473**, 222-226 (2000).
50. Li, W. *et al.* Star-PAP control of BIK expression and apoptosis is regulated by nuclear PIPKIalpha and PKCdelta signaling. *Mol Cell* **45**, 25-37 (2012).
51. Mellman, D.L. *et al.* A PtdIns4,5P2-regulated nuclear poly(A) polymerase controls expression of select mRNAs. *Nature* **451**, 1013-1017 (2008).
52. Tanaka, K. *et al.* Evidence that a phosphatidylinositol 3,4,5-trisphosphate-binding protein can function in nucleus. *Journal of Biological Chemistry* **274**, 3919-3922 (1999).
53. Wang, Y.H. *et al.* DNA damage causes rapid accumulation of phosphoinositides for ATR signaling. *Nat Commun* **8**, 2118 (2017).
54. Wang, Y.H. & Sheetz, M.P. When PIP(2) Meets p53: Nuclear Phosphoinositide Signaling in the DNA Damage Response. *Front Cell Dev Biol* **10**, 903994 (2022).
55. Wang, Y.H. & Sheetz, M.P. Transcription-independent functions of p53 in DNA repair pathway selection. *Bioessays* **45**, e2200122 (2023).
56. Barlow, C.A., Laishram, R.S. & Anderson, R.A. Nuclear phosphoinositides: a signaling enigma wrapped in a compartmental conundrum. *Trends Cell Biol* **20**, 25-35 (2010).
57. Cockcroft, S. & Carvou, N. Biochemical and biological functions of class I phosphatidylinositol transfer proteins. *Biochim Biophys Acta* **1771**, 677-691 (2007).
58. Li, F.L. *et al.* Hippo pathway regulation by phosphatidylinositol transfer protein and phosphoinositides. *Nat Chem Biol* **18**, 1076-1086 (2022).

59. Costes, S.V. *et al.* Automatic and quantitative measurement of protein-protein colocalization in live cells. *Biophys J* **86**, 3993-4003 (2004).
60. Schober, P., Boer, C. & Schwarte, L.A. Correlation Coefficients: Appropriate Use and Interpretation. *Anesth Analg* **126**, 1763-1768 (2018).
61. Asmari, M., Ratih, R., Alhazmi, H.A. & El Deeb, S. Thermophoresis for characterizing biomolecular interaction. *Methods* **146**, 107-119 (2018).

FIGURE LEGEND

Figure 1. Stress induces the nuclear localization of PITPs

a, Domains of PITP class I and II protein family members. PITD, PI transfer domain; FFAT, two phenylalanines in an acidic tract; DDHD, Asp-Asp-His-Asp motif; LNS2, Lipin/Nde1/Smp2 domain.

b-c, Confocal images of IF staining against PITPα/PITPβ/PITPNC1 and PI4,5P_2 in MDA-MB-231 cells treated with vehicle or 30 μM cisplatin for 24 h. The nuclei were counterstained by DAPI. The nuclear levels of PITPs and PI4,5P_2 were quantified by ImageJ (**c**). n=3, 15 cells from each independent experiment. See expanded images in Extended Data Fig. 1a.

d, Quantification of nuclear PITPα/PITPβ levels by IF staining in wild-type and mutant p53 expressing cells, including MCF10A (WT), A549 (WT), HCT116 (WT), BT-549 (R249S), Cal33 (R175H), HS578T (V157F), SUM159 (R158InL), and SUM1315 (C135F). n=3, 10 cells from each independent experiment. See IF images in Extended Data Fig. 2a.

e-f, MDA-MB-231 cells were treated with 30 μM cisplatin, 20 μM erastin, 100 μM tBHQ, 100 μM etoposide, 100 μM hydroxyurea, or vehicle for 24 h. The cells were then processed for IF staining against PITPα or PITPβ and PI4,5P_2. The nuclei were counterstained by DAPI. The nuclear levels of PITPs and PI4,5P_2 were quantified by ImageJ (**f**). n=3, 15 cells from each independent experiment. See expanded images in Extended Data Fig. 2b.

g, Confocal IF of PITPα or PITPβ overlaid with the nuclear envelope marker Lamin A/C in MCF10A, A549, MDA-MB-231, SUM1315, and BT-549 cells treated with vehicle or 30 μM cisplatin for 24 h. The nuclei were counterstained by DAPI.

For all panels, data are represented as mean ± SD, *p* value denotes two-sided paired t-test. Scale bar, 5 μm.

Figure 2. PITPs regulate the nuclear PIP_n pool in response to stress

a-b, MDA-MB-231 cells were transfected with control siRNAs or siRNAs against PITPα, PITPβ, PITPNC1, or both PITPα and PITPβ. After 24 h, cells were treated with 30 μM cisplatin or vehicle for 24 h before being processed for IF staining. The nuclear $PI4,5P_2$ level was quantified by ImageJ (**b**). n=3, 15 cells from each independent experiment. See KD validation in Fig. 5a.

c-d, MDA-MB-231 cells were transfected with control siRNAs or siRNAs against both PITPα and PITPβ. After 24 h, cells were treated with 30 μM cisplatin or vehicle for 24 h before being processed for IF staining against PI4P/$PI3,4,5P_3$ and the shared epitope of PITPα and PITPβ. The nuclei were counterstained by DAPI. The nuclear PI4P and PI3,4,5P3 levels were quantified by ImageJ (**d**). n=3, 15 cells from each independent experiment. See KD validation in Fig. 5a.

e-g, A549, BT-549, MCF10A, and SUM1315 cells were transfected with control siRNAs or siRNAs against both PITPα and PITPβ. After 24 h, cells were treated with 30 μM cisplatin or vehicle for 24 h before being processed for IF staining against $PI4,5P_2$ and the shared epitope of PITPα and PITPβ. The nuclei were counterstained by DAPI. The nuclear $PI4,5P_2$ levels were quantified by ImageJ (**g**). n=3, 15 cells from each independent experiment. See KD validation in Fig. 2e and expanded images in Extended Data Fig. 3e.

h, Models showing stress-induced nuclear translocation of PITPα/β to regulate nuclear PIP_n pools.

For all panels, data are represented as mean ± SD, *p* value denotes two-sided paired t-test. Scale bar, 5 μm.

Figure 3. PITPα/β bind p53 and their interaction is regulated by cellular stress

a-b, PLA of p53-PITPα/PITPβ/PITPNC1/PITPNM1/PITPNM2 in MDA-MB-231 cells treated with vehicle or 30 μM cisplatin for 24 h. The nuclear p53-PITP foci were quantified (**b**). n=3, 10 cells from each independent experiment. See PLA of p53-PITPNM1/PITPNM2 images in Extended Data Fig. 4a.

c, PLA of p53-PITPα/PITPβ/PITPNC1 overlaid with the nuclear envelope marker Lamin A/C in MDA-MB-231 cells treated with vehicle or 30 μM cisplatin for 24 h. The nuclei were counterstained by DAPI.

d-g, Co-IP of PITPα/PITPβ/Hsp27 with p53 from MDA-MB-231 cells treated with vehicle or 30 μM cisplatin for 24 h. PITPα IP-ed by p53 (**e**), PITPβ IP-ed by p53 (**f**), and Hsp27 IP-ed by p53 (**g**), as well as PITPNC1/PITPNM1/PITPNM2 were analyzed by WB. n=3 independent experiments.

h-k, Co-IP of p53/Hsp27/αB-crystallin (αBC) with the shared epitope of PITPα/β from MDA-MB-231 cells treated with vehicle or 30 μM cisplatin for 24 h. p53 IP-ed by PITPα/β (**i**), Hsp27 IP-ed by PITPα/β (**j**), and αBC IP-ed by PITPα/β (**k**) were analyzed by WB. n=3 independent experiments.

l-o, *In vitro* binding of recombinant p53 with PITPα or PITPβ. p53 immobilized on anti-p53 agarose was incubated with PITPα or PITPβ protein. p53 was IP'ed and p53-bound PITPα (**l**,**m**) or PITPβ (**n**,**o**) was analyzed by WB and quantified by ImageJ. n=3 independent experiments.

p, Model showing stress-induced formation of nuclear PITPα/β, p53, and small heat shock protein (sHSP) complexes.

For all panels, data are represented as mean ± SD, *p* value denotes two-sided paired t-test. Scale bar, 5 μm.

Figure 4. PITPα/β regulate the binding of PIP_ns with p53 in response to stress

a-c, MDA-MB-231 cells were transfected with control siRNAs or siRNAs against p53, PITPα, PITPβ, PITPNC1, or both PITPα and PITPβ. After 24 h, cells were treated with 30 μM cisplatin or vehicle for 24 h before being processed for PLA to detect p53-PI4,5P_2/-PI3,4,5P_3 complexes (**b,c**). n=3, 10 cells from each independent experiment. See KD validation in Fig. 5a and expanded images in Extended Data Fig. 6a,b.

d-f, A549 cells were transfected with control siRNAs or siRNAs against PITPα, PITPβ, or both PITPα and PITPβ. After 24 h, cells were treated with 30 μM cisplatin or vehicle for 24 h before being processed for PLA to detect p53-PI4,5P_2/PI3,4,5P_3 complexes (**e,f**). n=3, 10 cells from each independent experiment. See KD validation in Fig. 5b and expanded images in Extended Data Fig. 6c.

g, MDA-MB-231 cells were treated with 30 μM cisplatin or vehicle for 24 h before being processed for IP against p53. p53-bound PI4P/PI4,5P_2/PI3,4,5P_3 were examined by fluorescent WB. n=3 independent experiments. See quantification in Extended Data Fig. 6d.

h-k, MDA-MB-231 cells were transfected with control siRNAs or siRNAs against PITPα, PITPβ, or both PITPα and PITPβ. After 24 h, cells were treated with 30 μM cisplatin or vehicle for 24 h before being processed for IP against p53. p53-bound

PI4P/PI4,5P_2/PI3,4,5P_3 were examined by fluorescent WB and quantified by ImageJ (**i-k**)**.** n=3 independent experiments. See KD validation in Fig. 5a.

l-m, MDA-MB-231 cells were cultured from low confluency in media containing [^{3}H]*myo*-inositol or unlabeled *myo*-inositol. After 72 h of growth to confluency, cells were treated with 30 μM cisplatin or vehicle for 24 h before being processed for IP against p53. p53 and PI4,5P_2 were confirmed by flourecent WB (**l**) before samples were resolved by SDS-PAGE and the gel lane was excised and sectioned. Gel sections were then dissolved and analyzed by liquid scintillation counting (LSC) (**m**). n=3 independent experiments, error bar denotes SD, t-test, p<0.01*, p<0.001**

n-o, A549 cells were transfected with control siRNAs or siRNAs against PITPα, PITPβ, or both PITPα and PITPβ. After 24 h, cells were treated with 30 μM cisplatin or vehicle for 24 h before being processed for IP against p53. The PI4,5P_2 level on IPed p53 was quantified by ImageJ (**o**). n=3 independent experiments. See KD validation in Fig. 5b.

For all graphs, data are presented as the mean ± SD, and *p* values are from two-sided paired t-tests. Scale bar, 5 μm.

Figure 5. PITPα/β regulate p53 stability and PIP$_n$ linkage to protein targets

a, MDA-MB-231 cells were transfected with control siRNAs or siRNAs against p53, PITPα, PITPβ, PITPNC1, or both PITPα and PITPβ. After 24 h, cells were treated with 30 μM cisplatin or vehicle for 24 h before being processed for WB to validate the KD. The p53 level was quantified by ImageJ. n=3 independent experiments.

b, A549 cells were transfected with control siRNAs or siRNAs against PITPα, PITPβ, or both PITPα and PITPβ. After 24 h, cells were treated with 30 μM cisplatin or vehicle for

24 h before being processed for WB. The p53 level and protein-bound PI4,5P_2 level were quantified by ImageJ. n=3 independent experiments.

c-d, MDA-MB-231 cells were transfected with control siRNAs or siRNAs against p53, PITPα, PITPβ, PITPNC1, or both PITPα and PITPβ. After 24 h, cells were treated with 30 μM cisplatin or vehicle for 24 h before being processed for triple fluorescent WB for detecting p53 (Red), GAPDH (Blue), and protein-bound PI4,5P_2 (Green) simultaneously. The protein-bound PI4,5P_2 levels were quantified by ImageJ (**d**). See KD validation in Fig. 5a. n=3 independent experiments.

e-f, A549 cells were transfected with control siRNAs or siRNAs against PITPα or PITPβ. After 24 h, cells were treated with 30 μM cisplatin or vehicle for 24 h before being processed for WB. The protein-bound PIP_n levels were quantified by ImageJ (**f**). n=3 independent experiments.

g, MDA-MB-231 cells were cultured from low confluency in media containing in [^{3}H]*myo*-inositol or unlabeled *myo*-inositol. After 48 h, cells were transfected with control siRNAs or siRNAs against PITPα and PITPβ. 24 h later, cells were treated with 30 μM cisplatin or vehicle for another 24 h. KD and loading was confirmed by WB before the protein fraction was extracted with $CHCl_3$/MeOH or resolved by SDS-PAGE and the gel lane was excised. Extracted samples and dissolved gel sections were then analyzed by LSC. n=3 independent experiments. See expanded images in Extended Data Fig. 6h and experimental approach in Extended Data Fig. 6g.

For all graphs, data are presented as the mean ± SD, and *p* values are from two-sided paired t-tests.

Figure 6. PI4KIIα interacts with PITPα/β and p53 to generate p53-PIP_n complexes and stabilize p53

a-b, MDA-MB-231 cells were transfected with control siRNAs or siRNAs against PI4KIIIα, PI4KIIIβ, PI4KIIα, PI4KIIβ or both PI4KIIα and PI4KIIIα. After 24 h, cells were treated with 30 μM cisplatin or vehicle for 24 h before being processed for PLA to detect p53-PI4P complexes (**b**). n=3, 15 cells from each independent experiment. See KD confirmation in Fig. 6c and expanded images in Extended Data Fig. 6i.

c, MDA-MB-231 cells were transfected with control siRNAs or siRNAs against PI4KIIIα, PI4KIIIβ, PI4KIIα, PI4KIIβ or both PI4KIIα and PI4KIIIα. After 24 h, cells were treated with 30 μM cisplatin or vehicle for 24 h before being processed for WB. p53 levels were quantified by ImageJ. n=3 independent experiments.

d, A549 and MDA-MB-231 cells were transfected with control siRNAs or siRNAs against PI4KIIIα, PIPKIα or both PI4KIIα and PIPKIα. After 24 h, cells were treated with 30 μM cisplatin or vehicle for 24 h before being processed for WB. p53 levels were quantified by ImageJ. n=3 independent experiments.

e,f, MDA-MB-231 and A549 cells were transfected with control siRNAs or siRNAs against PI4KIIIα, PIPKIα or both PI4KIIα and PIPKIα. After 24 h, cells were treated with 30 μM cisplatin or vehicle for 24 h before being processed for PLA to detect p53-PI4P complexes. n=3, 15 cells from each independent experiment. See KD confirmation in Fig. 6d and expanded images in Extended Data Fig. 6j.

h, MDA-MB-231^{Cas9} cells with PITPβ KO and control non-targeted KO were transfected with control siRNAs or siRNAs against PI4KIIα, PITPα or both PI4KIIα and PITPα. After

24 h, cells were treated with 30 μM cisplatin or vehicle for 24 h before being processed for WB. n=3 independent experiments.

i, MDA-MB-231 cells were transfected with control siRNAs or siRNAs against PI4KIIα. After 24h, cells were treated with 30 μM cisplatin or vehicle for 24 h before being processed for PI4KIIα and PI4,5P_2 IF staining. n=3, 15 cells from each independent experiment. See expanded images in Extended Data Fig. 7f and quantification in Extended Data Fig. 7g.

j, Model showing PITPα/β cooperation with PI4KIIα in generating p53-PI4P complexes that participate in further signaling.

For all panels, data are represented as mean ± SD, *p* value denotes two-sided paired t-test. Scale bar, 5 μm.

Figure 7. PITPα/β regulate p53-dependent nuclear Akt activation and cell survival

a-b, MDA-MB-231 cells were transfected with control siRNAs or siRNAs against PITPα, PITPβ, PITPNC1, or both PITPα and PITPβ. After 24h, cells were treated with 30 μM cisplatin or vehicle for 24 h before being processed for IF staining against $pAkt^{S473}$. The nuclear $pAkt^{S473}$ levels were quantified by ImageJ (**b**). n=3, 15 cells from each independent experiment. Scale bar, 5 μm.

c-e, BT-549, SUM159, and SUM1315 cells with the indicated p53 status were transfected with control siRNAs or siRNAs against both PITPα and PITPβ. After 24 h, cells were treated with 30 μM cisplatin or vehicle for 24 h before being processed for IF staining against $pAkt^{S473}$. The nuclei were counterstained by DAPI. The nuclear $pAkt^{S473}$ levels were quantified (**d**). n=3, 15 cells from each independent experiment. Scale bar, 5 μm.

The double KD of PITPα and PITPβ in SUM159 cells was validated by WB (**e**). See KD validation for BT-549 and SUM1315 cells in Fig. 2e.

f-g, MDA-MB-231 cells were transfected with control siRNAs or siRNAs against p53, PITPα, PITPβ, PITPNC1, or both PITPα and PITPβ. After 24 h, cells were treated with 30 μM cisplatin or vehicle for 24 h before being processed for Crystal Violet viability assay. The cells were imaged by EVOS M5000 microscope (**f**) and quantified based on the extracted dye using a plate reader (**g**). Scale bar, 300 μm.

h, MDA-MB-231^{Cas9} cells with PITPβ KO and control non-targeted KO were transfected with control siRNAs or siRNAs against PITPα, PITPβ or both PITPα and PITPβ. After 24 h, cells were treated with 30 μM cisplatin or vehicle for 24 h before being processed for Crystal Violet viability assay. The cells were imaged by EVOS M5000 microscope. Scale bar, 300 μm. n=3 independent experiments. See quantification in Extended Data Fig. 7h.

i, MDA-MB-231 cells were transfected with control siRNAs or siRNAs against p53, PITPα, PITPβ, PITPNC1, or both PITPα and PITPβ. After 24h, cells were treated with 30 μM cisplatin or vehicle for 24 h before being processed for caspase 3 activity assay. n=3 independent experiments.

For all graphs, data are presented as the mean ± SD, and *p* values are from two-sided paired t-tests.

Figure 8. PITPα/β initiate the p53-PIP$_n$ signalosome by a PI binding-dependent mechanism

a, HEK293FT cells were co-transfected with either HA-tagged wild-type PITPα or PI binding-defective mutant T59D PITPα together with Flag-tagged p53^{wt}. After 48 h, cells

were processed for IP against Flag-tag and analyzed by WB. n=3 independent experiments.

b-e, MDA-MB-231 cells were transfected with control siRNAs or siRNAs against the 3'UTR of both PITPα and PITPβ for 24 h. Then the cells were transfected with either HA-tagged wild-type PITPα/β or PI binding-defective mutant T59D PITPα/β. After 24 h, cells were treated with 30 μM cisplatin or vehicle for 24 h before being processed for WB (**b**) and IF staining against HA-tag with $PI4,5P_2$ or $pAkt^{S473}$ (**c**). The nuclear $PI4,5P_2$ and $pAkt^{S473}$ levels in HA-positive cells were quantified by ImageJ (**d, e**). n=3, 15 cells from each independent experiment. Scale bar, 5 μm.

f-i, Pearson's correlation coefficient (Pearson's r) quantified the correlations between nuclear $PI4,5P_2$ or $pAkt^{S473}$ with HA-$PITP\alpha^{wt/T59D}$ levels. n=100 cells pooled from 3 independent experiments.

j-k, MDA-MB-231 cells were transfected with control siRNAs or siRNAs against the 3'UTR of both PITPα and PITPβ for 24 h. The cells were then transfected with either HA-tagged wild-type PITPα or PI binding-defective mutant T59D PITPα. After 24 h, cells were treated with 30 μM cisplatin or vehicle for 24 h before being processed for Crystal Violet viability assay. The cells were imaged by EVOS M5000 microscope (**j**) and quantified based on the extracted dye using a plate reader (**k**). n=3 independent experiments. Scale bar, 300 μm.

l-m, MDA-MB-231 cells were transfected with control siRNAs or siRNAs against the 3'UTR of both PITPα and PITPβ for 24 h. The cells were then transfected with either HA-tagged wild-type PITPα or PI binding-defective mutant T59D PITPα. After 24 h, cells were serum starved for an additional 24 h and then scored for invasion through Laminin-coated

transwell inserts with 8 μm pores using 10 ng/ml EGF as a chemoattractant for 16 h. The invading cells at the insert bottom were stained with Crystal Violet, imaged (**l**), and quantified (**m**) based on the extracted dye using a plate reader. n=3 independent experiments. Scale bar, 300 μm.

n, A model of the stress-induced nuclear accumulation of class I PITPs and PITP-dependent initiation of the p53-PI signalosome which promotes cell proliferation, survival, and invasion.

For all graphs, data are presented as the mean ± SD, and *p* values are from two-sided paired t-tests.

SUPLEMENTAL INFORMATION

Extended Data Figure 1. Cisplatin induces the nuclear accumulation of PITPs

a, Confocal images of IF staining against PITPα/PITPβ/PITPNC1 and PI4,5P_2 in MDA-MB-231 cells treated with vehicle or 30 μM cisplatin for 24 h. The nuclei were counterstained by DAPI. See quantification in Fig. 1c.

b-c, 3D sections of IF staining against PITPα in MDA-MB-231 cells treated with vehicle or 30 μM cisplatin for 24 h. The nuclei were counterstained by DAPI. Each frame of the 3D sections was over a 0.2 μm thickness.

d-e, 3D sections of IF staining against PITPβ in MDA-MB-231 cells treated with vehicle or 30 μM cisplatin for 24 h. The nuclei were counterstained by DAPI. Each frame of the 3D sections was over a 0.2 μm thickness.

For all panels, Scale bar, 5 μm.

Extended Data Figure 2. Diverse cellular stressors induce the nuclear localization of PITPs in multiple cell lines

a, Confocal images of the IF staining against PITPα/β in wild-type and mutant p53 expressing cells, including MCF10A (WT), A549 (WT), HCT116 (WT), BT-549 (R249S), Cal33 (R175H), HS578T (V157F), SUM159 (R158lnL), and SUM1315 (C135F). The nuclei were counterstained by DAPI. See the quantification of the nuclear levels of PITPα/PITPβ in Fig. 1d.

b, MDA-MB-231 cells treated with 30 μM cisplatin, 20 μM erastin, 100 μM tBHQ, 100 μM etoposide, 100 μM hydroxyurea, or vehicle for 24 h. The cells were processed for IF staining against PITPα and PI4,5P_2. The nuclei were counterstained by DAPI. See the quantification of nuclear PITPα, PITPβ and PI4,5P_2 in Fig. 1f.

c, Confocal IF of PITPNC1 overlaid with the nuclear envelope marker Lamin A/C in MDAMB-231 and A549 cells treated with vehicle or 30 μM cisplatin for 24 h. The nuclei were counterstained by DAPI.

For all panels, Scale bar, 5 μm.

Extended Data Figure 3. PITPs regulate the non-membranous PI4,5P_2 pools in the nucleus

a-d, Confocal IF images of PITPα/β overlaid with the nuclear envelope marker Lamin A/C in wild-type and mutant p53 expressing cancer cells, including HCT116 (WT, **a**), Cal33 (R175H, **b**), HS578T (V157F, **c**), and SUM159 (R158lnL, **d**). The nuclei were counterstained by DAPI.

e, MCF10A and SUM1315 cells with the indicated p53 status were transfected with control siRNAs or siRNAs against both PITPα and PITPβ. After 24 h, cells were treated

with 30 μM cisplatin or vehicle for 24 h before being processed for IF staining against $PI4,5P_2$ and the shared epitope of PITPα and PITPβ. The nuclei were counterstained by DAPI. See KD validation in Fig. 2e and quantification in Fig. 2g. n=3, 15 cells from each independent experiment.

For all panels, Scale bar, 5 μm.

Extended Data Figure 4. Stress induces PITPα/β association with p53 in the non-membranous nucleoplasm

a, PLA of p53-PITPNM1/PITPNM2 in MDA-MB-231 cells treated with vehicle or 30 μM cisplatin for 24 h. See quantification in Fig. 3b.

b-c, PLA of p53-PITPα/PITPβ/PITPNC1/PITPNM1/PITPNM2 in A549 cells treated with vehicle or 30 μM cisplatin for 24 h. The nuclear p53-PITP PLA foci were quantified by ImageJ (**c**). n=3, 10 cells from each independent experiment.

d, PLA of p53-PITPα/PITPβ/PITPNC1/PITPNM1/PITPNM2 overlaid with the nuclear envelope marker Lamin A/C in A549 cells treated with vehicle or 30 μM cisplatin for 24 h. The nuclei were counterstained by DAPI.

e, PLA of p53-PITPNM1/PITPNM2 overlaid with the nuclear envelope marker Lamin A/C in MDA-MB-231 treated with vehicle or 30 μM cisplatin for 24 h. The nuclei were counterstained by DAPI.

f, 3D sections of p53-PITPβ PLA foci overlaid with Lamin A/C in MDA-MB-231 treated with vehicle or 30 μM cisplatin for 24 h. The nuclei were counterstained by DAPI. Each frame of the 3D sections was over a 0.2 μm thickness.

For all panels, data are represented as mean ± SD, *p* value denotes two-sided paired t-test. Scale bar, 5 μm unless otherwise indicated.

Extended Data Figure 5. Stress induces PITPα/β association with p53

a-d, Co-IP of p53/Hsp27/αB-crystallin (αBC) with the shared epitope of PITPα/β in MCF10A cells treated with vehicle or 30 μM cisplatin for 24 h. p53 immunoprecipitated (IPed) by PITPα/β (**b**), Hsp27 IPed by PITPα/β (**c**), and αBC IPed by PITPα/β (**d**) were analyzed by WB. n=3 independent experiments.

e-f, Co-IP of p53 with the shared epitope of PITPα/β in A549 cells treated with vehicle or 30 μM cisplatin for 24 h. p53 IPed by PITPα/β was analyzed by WB (**f**). n=3 independent experiments.

g-h, Co-IP of p53 with the shared epitope of PITPα/β in HCT116 cells treated with vehicle or 30 μM cisplatin for 24 h. p53 IPed by PITPα/β was analyzed by WB (**h**). n=3 independent experiments.

i-n, Co-IP of PITPα/PITPβ with p53 in BT549, Cal33, HS578T, SUM159, SUM1315 cells treated with vehicle or 30 μM cisplatin for 24 h. PITPα/PITPβ IPed by p53 (**n**) as well as PITPNC1/PITPNM1/PITPNM2 were analyzed by WB. n=3 independent experiments.

For all panels, data are represented as mean ± SD, *p* value denotes two-sided paired t-test.

Extended Data Figure 6. PITPα/β and PI4KIIα regulate p53-PIP$_n$ signaling in response to stress

a-b, MDA-MB-231 cells were transfected with control siRNAs or siRNAs against p53, PITPα, PITPβ, PITPNC1, or both PITPα and PITPβ. After 24 h, cells were treated with 30 μM cisplatin or vehicle for 24 h before being processed for PLA to detect p53-PI4,5P$_2$ (**a**) and p53-PI3,4,5P$_3$ (**b**) complexes. n=3 independent experiments. See KD validation in Fig. 5a, expanded images in Fig. 4a, and quantification in Fig. 4b,c.

c, A549 cells were transfected with control siRNAs or siRNAs against PITPα, PITPβ, or both PITPα and PITPβ. After 24 h, cells were treated with 30 μM cisplatin or vehicle for 24 h before being processed for PLA to detect p53-PI4,5P_2/PI3,4,5P_3 complexes. n=3 independent experiments. See KD validation in Fig. 5b, expanded images in Fig. 4d, and quantification in Fig. 4e,f.

d, MDA-MB-231 cells were treated with 30 μM cisplatin or vehicle for 24 h before being processed for IP against p53. p53-bound PI4P/PI4,5P_2/PI3,4,5P_3 were examined by fluorescent WB in Fig. 4g. n=3 independent experiments.

e, MDA-MB-231 cells were treated with 30 μM cisplatin and lysates were made at the indicated timpoints along a 24 h timecourse. Whole cell lysates were then processed for WB.

f, MDA-MB-231^{Cas9} cells with PITPβ KO and control non-targeted KO were transfected with control siRNAs or siRNAs against PITPα, PITPβ or both PITPα and PITPβ. After 24 h, cells were treated with 30 μM cisplatin or vehicle for 24 h before being processed for WB. n=3 independent experiments.

g-h, MDA-MB-231 cells were cultured from low confluency in media containing [^{3}H]*myo*-inositol or unlabeled myo-inositol. After 48 h, cells were transfected with control siRNAs or siRNAs against PITPα and PITPβ. 24 h later, cells were treated with 30 μM cisplatin or vehicle for another 24 h. KD and loading was confirmed by WB. Dissolved gel sections were then analyzed by LSC (**g**). n=3 independent experiments. See expanded images and LSC quantification in Fig. 5g.

i, MDA-MB-231 cells were transfected with control siRNAs or siRNAs against PI4KIIIα, PI4KIIIβ, PI4KIIα, PI4KIIβ or both PI4KIIα and PI4KIIIα. After 24 h, cells were treated with

30 μM cisplatin or vehicle for 24 h before being processed for PLA to detect p53-PI4P complexes. n=3, 15 cells from each independent experiment. See KD confirmation in Fig. 6c, expanded images in Fig. 6a, and quantification in Fig. 6b.

j, MDA-MB-231 and A549 cells were transfected with control siRNAs or siRNAs against PI4KIIIα, PIPKIα or both PI4KIIα and PIPKIα. After 24 h, cells were treated with 30 μM cisplatin or vehicle for 24 h before being processed for PLA to detect p53-PI4P complexes. n=3, 15 cells from each independent experiment. See KD confirmation in Fig. 6d, expanded images in Fig. 6e, and quantification in Fig. 6f.

For all panels, data are represented as mean ± SD, *p* value denotes two-sided paired t-test.

Extended Data Figure 7. PI4KIIα interacts with PITPα/β and p53 to promote p53-PIP_n and protein-PIP_n signaling

a-c, *In vitro* binding of recombinant PI4KIIα and p53 (**a**), PI4KIIα and PITPα (**b**) and PI4KIIα and PITPβ (**c**). p53, PITPα or PITPβ immobilized on the indicated antibody-conjugated agarose was incubated with PI4KIIα protein. p53, PITPα or PITPβ was IPed and p53-bound PI4KIIα (**a**), PITPα-bound PI4KIIα (**b**) and PITPβ-bound PI4KIIα (**c**) was analyzed by WB and quantified by ImageJ. n=3 independent experiments.

d, MDA-MB-231 cells were transfected with control siRNAs or siRNAs against both PITPα and PITPβ or PI4KIIα. After 24 h, cells were treated with 30 μM cisplatin or vehicle for 24 h before being processed for WB. n=3 independent experiments.

e, MDA-MB-231^{Cas9} cells with PITPβ KO and control non-targeted KO were transfected with control siRNAs or siRNAs against PI4KIIα, PITPα or both PI4KIIα and PITPα. After

24 h, cells were treated with 30 μM cisplatin or vehicle for 24 h before being processed for WB. n=3 independent experiments.

f-g, MDA-MB-231 cells were transfected with control siRNAs or siRNAs against PI4KIIα. After 24h, cells were treated with 30 μM cisplatin or vehicle for 24 h before being processed for IF staining. The nuclear PI4,5P_2 level was quantified by ImageJ (**g**). n=3, 15 cells from each independent experiment. See expanded images in Fig. 6i.

h, MDA-MB-231^{Cas9} cells with PITPβ KO and control non-targeted KO were transfected with control siRNAs or siRNAs against PITPα, PITPβ or both PITPα and PITPβ. After 24 h, cells were treated with 30 μM cisplatin or vehicle for 24 h before being processed for Crystal Violet viability assay. Viability was quantified based on the extracted dye using a plate reader. n=3 independent experiments. See representative images in Fig. 7h.

For all panels, data are represented as mean ± SD, *p* values are from two-sided paired t-tests.

Extended Data Figure 8. PITPα/β and mutant p53 inhibit genotoxic stress-induced apoptosis

a-g, BT-549, SUM159, and SUM1315 cells were transfected with control siRNAs or siRNAs against p53, PITPα, PITPβ, or both PITPα and PITPβ. After 24 h, cells were treated with 30 μM cisplatin or vehicle for 24 h before being processed for Crystal Violet viability assay. The cells were imaged by EVOS M5000 microscope (**a**) and quantified based on the extracted dye using a plate reader (**b-d**). The KD was validated by WB (**e-g**). n=3 independent experiments.

h-j, BT-549, SUM159, and SUM1315 cells were transfected with control siRNAs or siRNAs against p53, PITPα, PITPβ, or both PITPα and PITPβ. After 24 h, cells were

treated with 30 μM cisplatin or vehicle for 24 h before being processed for caspase 3 activity assay. n=3 independent experiments.

For all graphs, data are presented as the mean ± SD, and *p* values are from two-sided paired t-tests. Scale bar, 300 μm.

k, HEK293FT cells were co-transfected with either HA-tagged wild-type PITPα or PI binding-defective mutant T59D PITPα together with Flag-tagged mutant $p53^{R175H}$. After 48 h, cells were processed for IP against Flag-tag and analyzed by WB. n=3 independent experiments.

l, HEK293FT cells were co-transfected with either HA-tagged wild-type PITPβ or PI binding-defective mutant T59D PITPβ together with Flag-tagged $p53^{wt}$. After 48 h, cells were processed for IP against Flag-tag and analyzed by WB. n=3 independent experiments.

m, HEK293FT cells were co-transfected with either HA-tagged wild-type PITPβ or PI binding-defective mutant T59D PITPβ together with Flag-tagged mutant $p53^{R175H}$. After 48 h, cells were processed for IP against Flag-tag and analyzed by WB. n=3 independent experiments.

n, MDA-MB-231 cells were transfected with control siRNAs or siRNAs against the 3'UTR of both PITPα and PITPβ for 24 h. The cells were then transfected with either HA-tagged wild-type PITPα or PI binding-defective mutant T59D PITPα. After 24 h, cells were treated with 30 μM cisplatin or vehicle for 24 h before being processed for caspase 3 activity assay. n=3 independent experiments.

For all graphs, data are presented as the mean ± SD, and *p* values are from two-sided paired t-tests. Scale bar, 300 μm.

Table 1. Binding affinities of p53-PIP_n signalisome componants

The binding affinity of the protein-PIP_n complex regulators and p53. The interaction of recombinant fluorescently labelled p53, PI4KIIα, and PITPβ with other components was quantitated by MST assay. A constant concentration of fluorescently labelled p53, PI4KIIα, or PITPβ (target, 5 nM) was incubated with increasing concentrations of non-labelled binding partners or ligands to calculate the binding affinity. The binding affinities determined by MST are shown as indicated K_d values. MST was performed using a Monolith NT.115 pico, and the binding affinity was autogenerated by MO. Control v.1.6 software. Data are presented as the mean ± SD; n = 3.

Supplementary Video 1

3D reconstitution of the p53-PITPβ complex in the nucleoplasm of MDA-MB-231 cells under basal conditions

MDA-MB-231 cells were treated with control vehicle for 24 h before being processed for PLA between p53 and PITPβ (Red). Lamin A/C stained the nuclear envelope (Green), and the nuclei were counter-stained with DAPI (Blue). The z-stack images were taken with a Leica SP8 confocal microscope with each frame over a 0.2 μm thickness. The video of the 3D reconstitution of a representative cell from three independent experiments was generated by LASX.

Supplementary Video 2

3D reconstitution of the p53-PITPβ complex in the nucleoplasm of MDA-MB-231 cells under stress

MDA-MB-231 cells were treated with 30 μM cisplatin for 24 h before being processed for PLA between p53 and PITPβ (Red). Lamin A/C stained the nuclear envelope (Green), and the nuclei were counter-stained with DAPI (Blue). The z-stack images were taken with a Leica SP8 confocal microscope with each frame over a 0.2 μm thickness. The video of the 3D reconstitution of a representative cell from three independent experiments was generated by LASX.

Table 1

	Binding Affinity Kd (nM)		
Target Protein	**p53**	**PI4KIIα**	**PITPβ**
PITPβ	19 ± 2	263 ± 12	-
PITPβ + PI (1μM)	5 ± 1	113 ± 11	-
p53	-	8 ± 1	15 ± 1
PI4KIIα	4 ± 1	-	201 ± 2

"-" denotes values that were not tested

Fig. 1

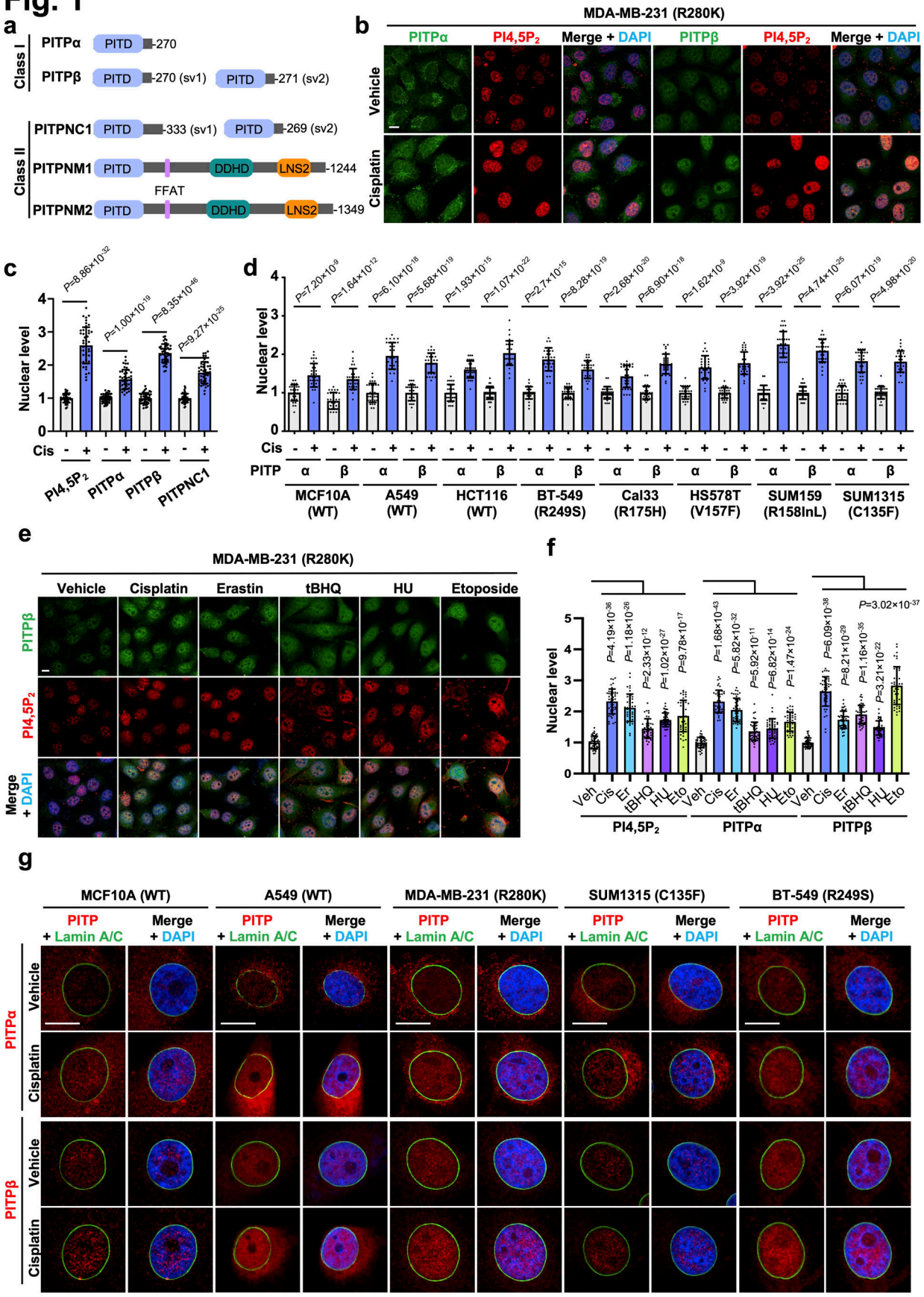
a
Class I
PITPα
PITD
-270
PITPβ
PITD
-270 (sv1)
PITD
-271 (sv2)
Class II
PITPNC1
PITD
-333 (sv1)
PITD
-269 (sv2)
PITPNM1
PITD
DDHD
LNS2
-1244
FFAT
PITPNM2
PITD
DDHD
LNS2
-1349
b
MDA-MB-231 (R280K)
PITPα
PI4,5P2
Merge + DAPI
PITPβ
PI4,5P2
Merge + DAPI
Vehicle
Cisplatin
c
Nuclear level
P=8.86×10-32
P=1.00×10-19
P=8.35×10-46
P=9.27×10-25
Cis
PI4,5P2
PITPα
PITPβ
PITPNC1
d
Nuclear level
P=7.20×10-9
P=1.64×10-12
P=6.10×10-18
P=5.68×10-19
P=1.93×10-15
P=1.07×10-22
P=2.7×10-15
P=8.28×10-19
P=2.68×10-20
P=6.90×10-18
P=1.62×10-9
P=3.92×10-19
P=3.92×10-25
P=4.74×10-25
P=6.07×10-19
P=4.98×10-20
Cis
PITP
MCF10A (WT)
A549 (WT)
HCT116 (WT)
BT-549 (R249S)
Cal33 (R175H)
HS578T (V157F)
SUM159 (R158lnL)
SUM1315 (C135F)
e
MDA-MB-231 (R280K)
Vehicle
Cisplatin
Erastin
tBHQ
HU
Etoposide
PITPβ
PI4,5P2
Merge + DAPI
f
Nuclear level
P=4.19×10-36
P=1.18×10-26
P=2.33×10-12
P=1.02×10-27
P=9.78×10-17
P=1.68×10-43
P=5.82×10-32
P=5.92×10-11
P=6.82×10-14
P=1.47×10-24
P=6.09×10-38
P=8.21×10-29
P=1.16×10-35
P=3.21×10-22
P=3.02×10-37
Veh
Cis
Er
tBHQ
HU
Eto
PI4,5P2
PITPα
PITPβ
g
MCF10A (WT)
A549 (WT)
MDA-MB-231 (R280K)
SUM1315 (C135F)
BT-549 (R249S)
PITP + Lamin A/C
Merge + DAPI
PITPα
PITPβ
Vehicle
Cisplatin

Fig. 2

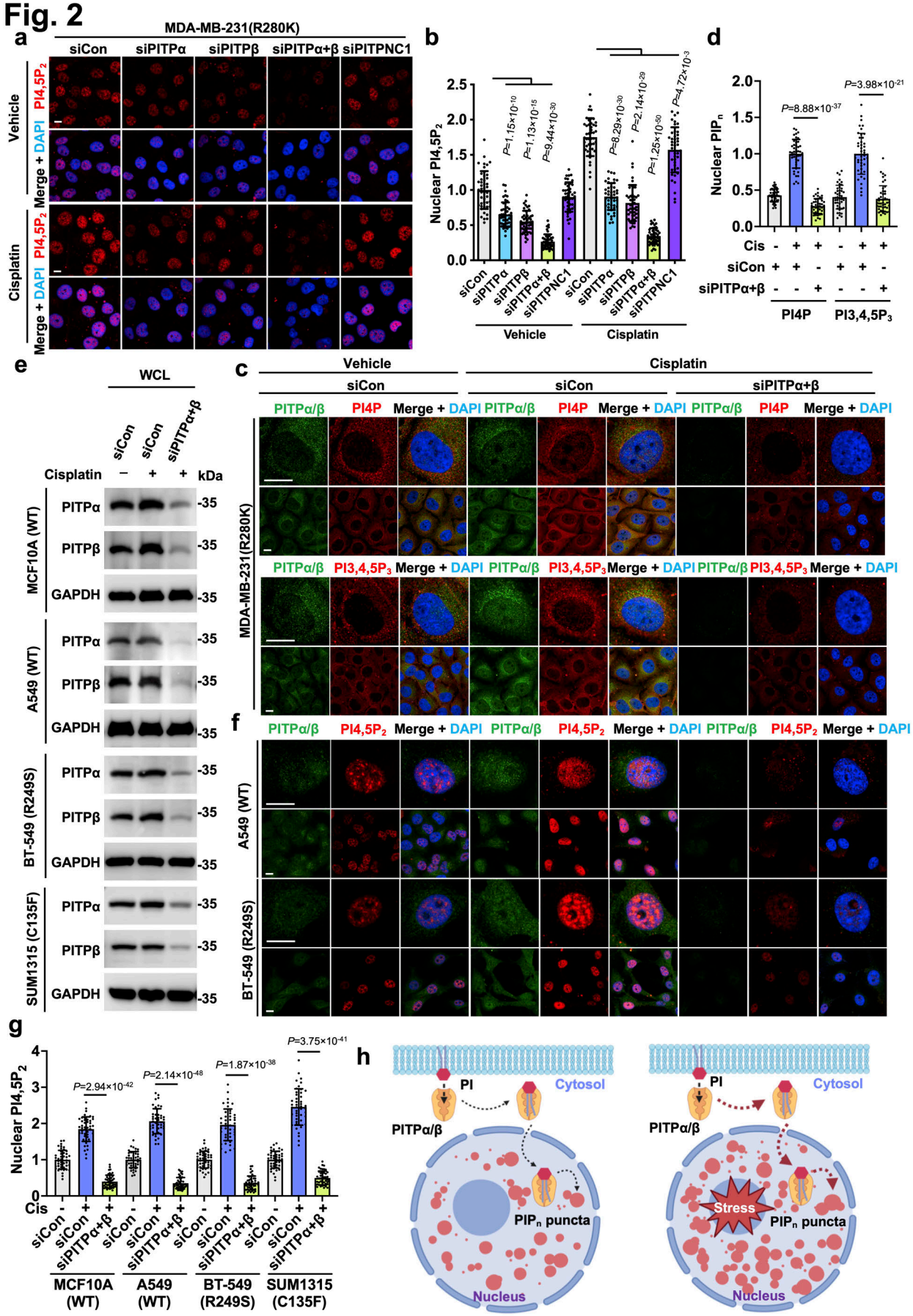
a
MDA-MB-231(R280K)
siCon
siPITPα
siPITPβ
siPITPα+β
siPITPNC1
Vehicle
Cisplatin
PI4,5P2
Merge + DAPI
b
Nuclear PI4,5P2
P=1.15×10-10
P=1.13×10-15
P=9.44×10-30
P=8.29×10-30
P=2.14×10-29
P=1.25×10-50
P=4.72×10-3
Vehicle
Cisplatin
d
Nuclear PIPn
P=8.88×10-37
P=3.98×10-21
Cis
siCon
siPITPα+β
PI4P
PI3,4,5P3
e
WCL
Cisplatin
kDa
MCF10A (WT)
A549 (WT)
BT-549 (R249S)
SUM1315 (C135F)
PITPα
PITPβ
GAPDH
-35
c
Vehicle
Cisplatin
siCon
siPITPα+β
PITPα/β
PI4P
PI3,4,5P3
Merge + DAPI
MDA-MB-231(R280K)
f
PI4,5P2
A549 (WT)
BT-549 (R249S)
g
Nuclear PI4,5P2
P=2.94×10-42
P=2.14×10-48
P=1.87×10-38
P=3.75×10-41
Cis
MCF10A (WT)
A549 (WT)
BT-549 (R249S)
SUM1315 (C135F)
h
PI
Cytosol
PITPα/β
PIPn puncta
Nucleus
Stress

Fig. 3

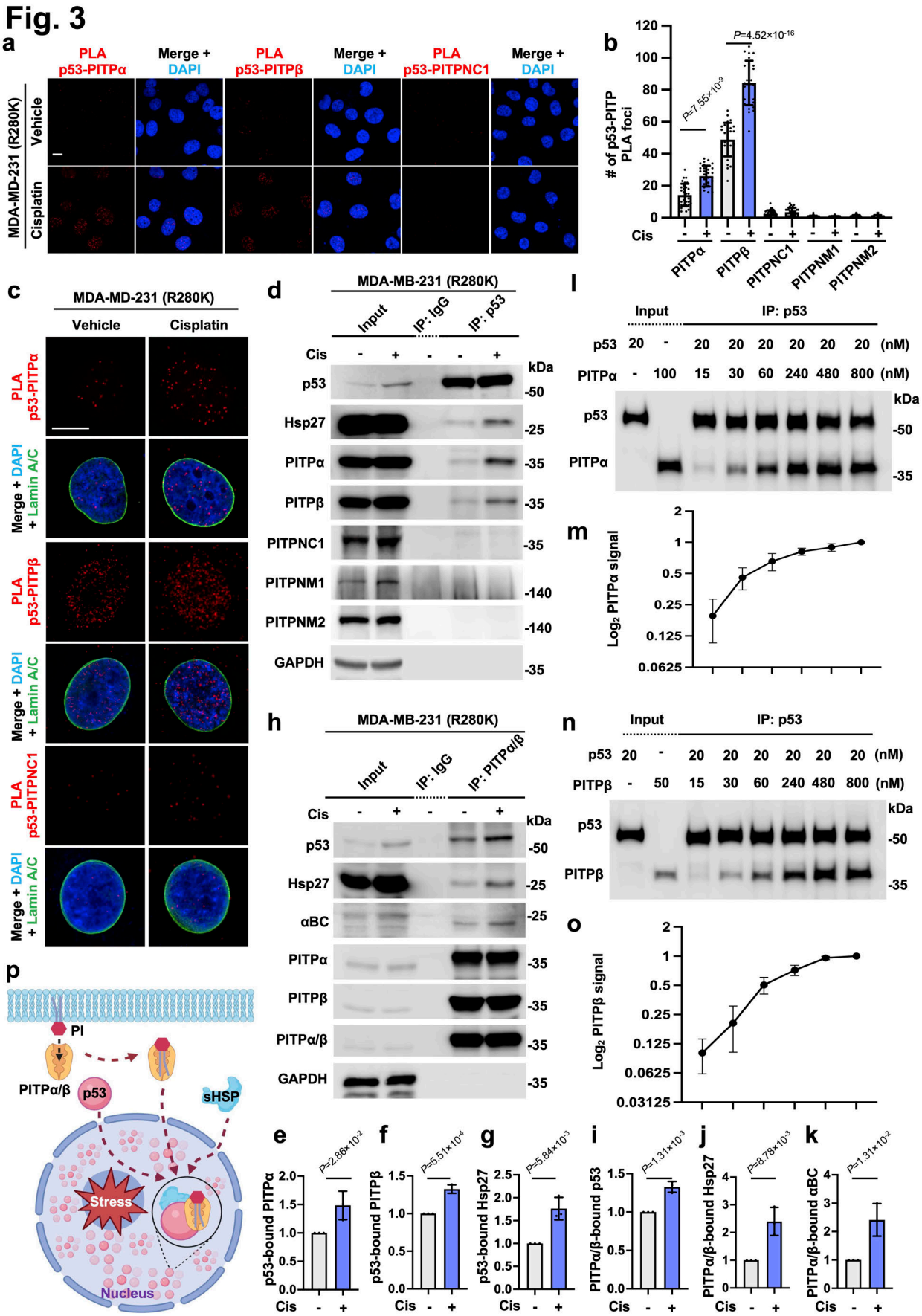
a
PLA p53-PITPα
Merge + DAPI
PLA p53-PITPβ
PLA p53-PITPNC1
MDA-MD-231 (R280K)
Vehicle
Cisplatin
b
# of p53-PITP PLA foci
P=7.55×10^-9
P=4.52×10^-16
Cis
PITPα
PITPβ
PITPNC1
PITPNM1
PITPNM2
c
MDA-MD-231 (R280K)
Vehicle
Cisplatin
PLA p53-PITPα
Merge + DAPI + Lamin A/C
PLA p53-PITPβ
PLA p53-PITPNC1
d
MDA-MB-231 (R280K)
Input
IP: IgG
IP: p53
Cis
kDa
p53
Hsp27
PITPα
PITPβ
PITPNC1
PITPNM1
PITPNM2
GAPDH
l
Input
IP: p53
p53 20 - 20 20 20 20 20 20 (nM)
PITPα - 100 15 30 60 240 480 800 (nM)
m
Log2 PITPα signal
h
MDA-MB-231 (R280K)
IP: PITPα/β
αBC
PITPα/β
n
p53 20 - 20 20 20 20 20 20 (nM)
PITPβ - 50 15 30 60 240 480 800 (nM)
o
Log2 PITPβ signal
p
PI
PITPα/β
p53
sHSP
Stress
Nucleus
e
p53-bound PITPα
P=2.86×10^-2
f
p53-bound PITPβ
P=5.51×10^-4
g
p53-bound Hsp27
P=5.84×10^-3
i
PITPα/β-bound p53
P=1.31×10^-3
j
PITPα/β-bound Hsp27
P=8.78×10^-3
k
PITPα/β-bound αBC
P=1.31×10^-2

Fig. 4

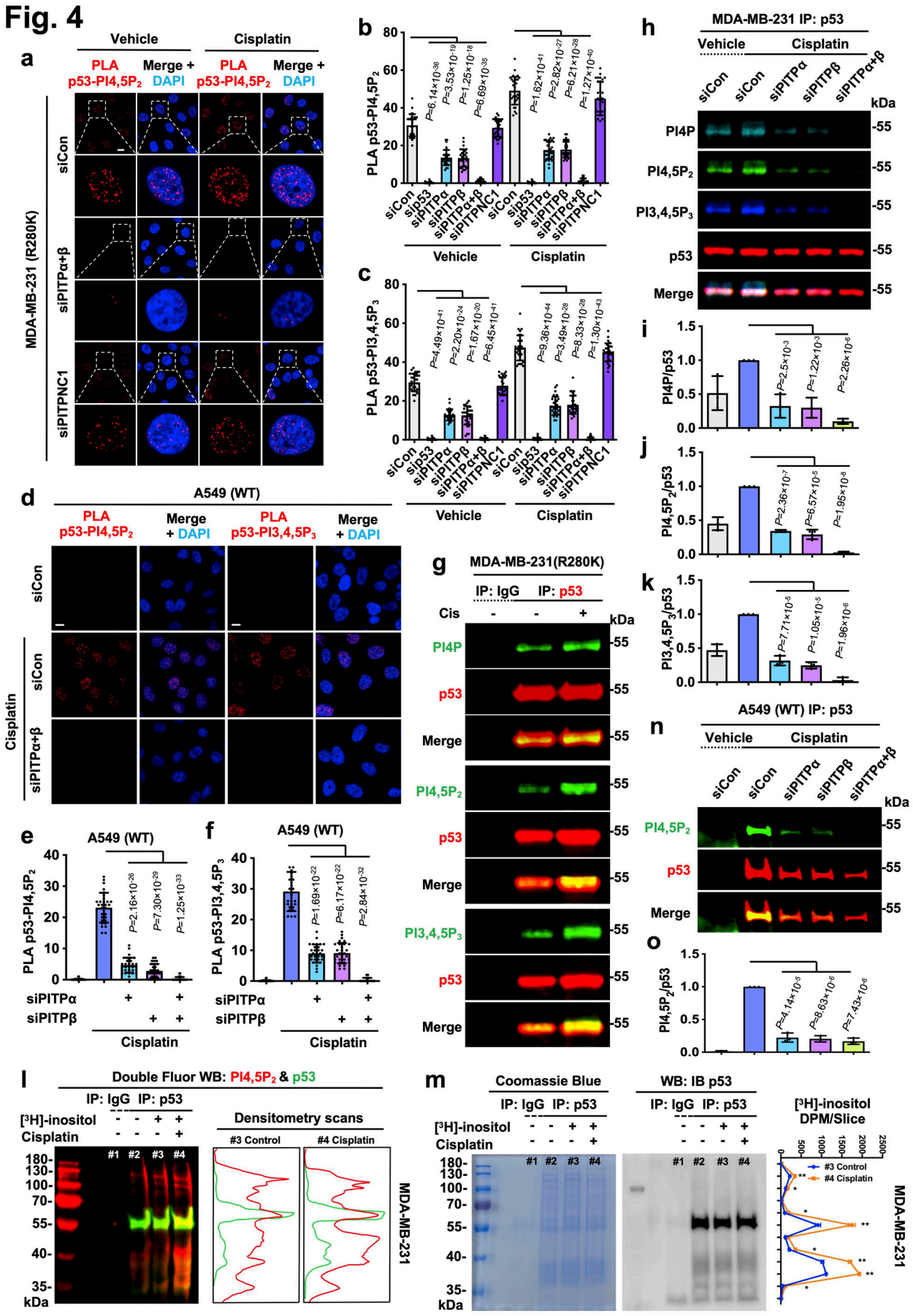
a
Vehicle
Cisplatin
PLA p53-PI4,5P2
Merge + DAPI
MDA-MB-231 (R280K)
siCon
siPITPα+β
siPITPNC1
b
PLA p53-PI4,5P2
P=6.14×10-36
P=3.53×10-19
P=1.25×10-18
P=6.69×10-35
P=1.62×10-41
P=2.82×10-27
P=6.21×10-28
P=1.27×10-40
siCon
sip53
siPITPα
siPITPβ
siPITPα+β
siPITPNC1
Vehicle
Cisplatin
c
PLA p53-PI3,4,5P3
P=4.49×10-41
P=2.20×10-24
P=1.67×10-20
P=6.45×10-41
P=9.36×10-44
P=3.49×10-28
P=8.33×10-28
P=1.30×10-43
d
A549 (WT)
PLA p53-PI4,5P2
Merge + DAPI
PLA p53-PI3,4,5P3
Merge + DAPI
siCon
Cisplatin
siPITPα+β
e
A549 (WT)
PLA p53-PI4,5P2
P=2.16×10-26
P=7.30×10-29
P=1.25×10-33
siPITPα
siPITPβ
Cisplatin
f
A549 (WT)
PLA p53-PI3,4,5P3
P=1.69×10-32
P=6.17×10-32
P=2.84×10-32
siPITPα
siPITPβ
Cisplatin
g
MDA-MB-231(R280K)
IP: IgG
IP: p53
Cis
kDa
PI4P
p53
Merge
PI4,5P2
PI3,4,5P3
55
h
MDA-MB-231 IP: p53
Vehicle
Cisplatin
siCon
siPITPα
siPITPβ
siPITPα+β
kDa
PI4P
PI4,5P2
PI3,4,5P3
p53
Merge
55
i
PI4P/p53
P=2.5×10-3
P=1.22×10-3
P=2.26×10-8
j
PI4,5P2/p53
P=2.36×10-7
P=6.57×10-5
P=1.95×10-8
k
PI3,4,5P3/p53
P=7.71×10-5
P=1.05×10-5
P=1.96×10-6
n
A549 (WT) IP: p53
Vehicle
Cisplatin
siCon
siPITPα
siPITPβ
siPITPα+β
kDa
PI4,5P2
p53
Merge
55
o
PI4,5P2/p53
P=4.14×10-5
P=8.63×10-6
P=7.43×10-6
l
Double Fluor WB: PI4,5P2 & p53
IP: IgG
IP: p53
[3H]-inositol
Cisplatin
#1
#2
#3
#4
kDa
Densitometry scans
#3 Control
#4 Cisplatin
MDA-MB-231
m
Coomassie Blue
WB: IB p53
IP: IgG
IP: p53
[3H]-inositol
Cisplatin
[3H]-inositol DPM/Slice
#3 Control
#4 Cisplatin
MDA-MB-231

Fig. 5

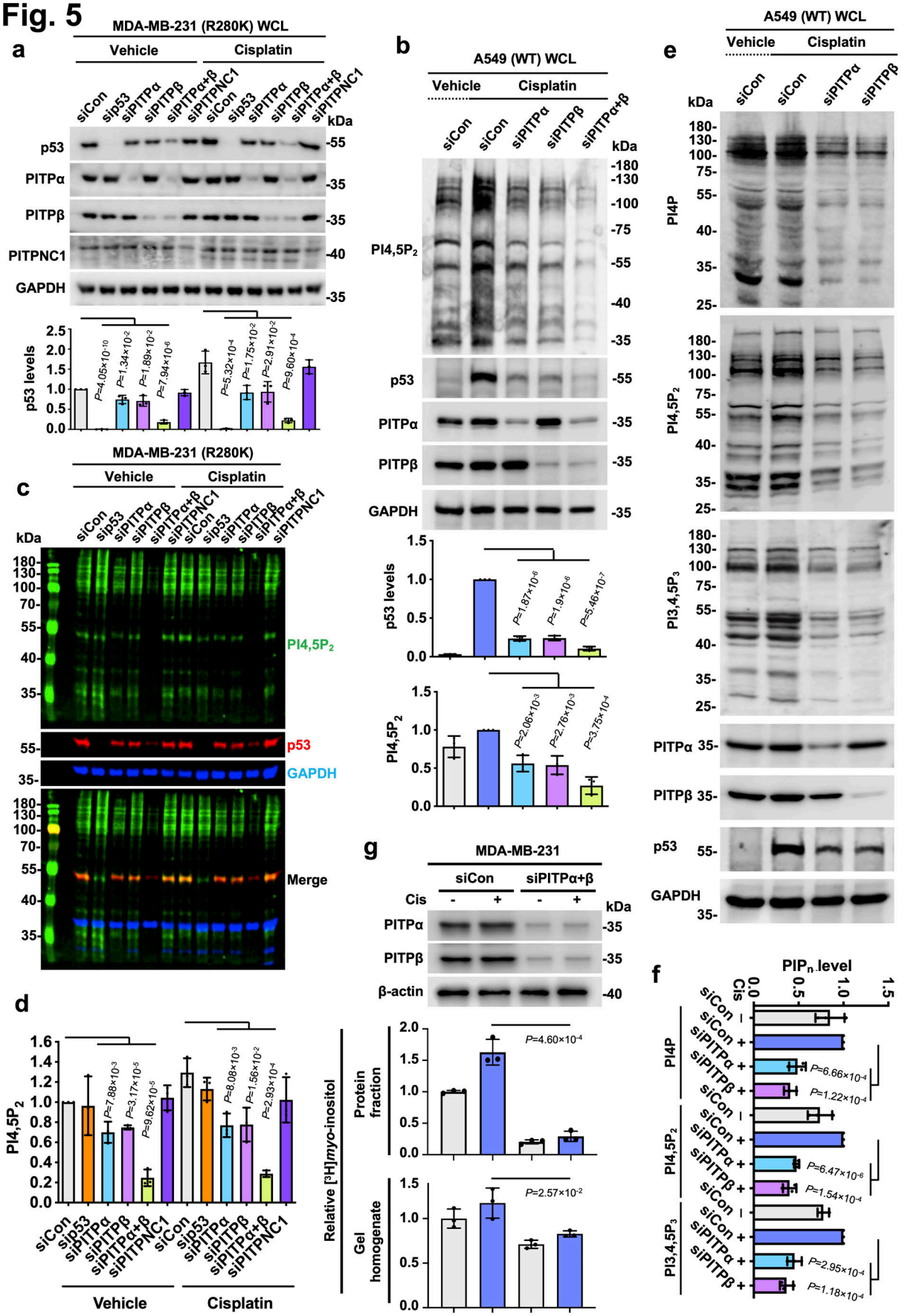
a
MDA-MB-231 (R280K) WCL
Vehicle
Cisplatin
siCon
sip53
siPITPα
siPITPβ
siPITPα+β
siPITPNC1
kDa
p53
PITPα
PITPβ
PITPNC1
GAPDH
p53 levels
P=4.05×10-10
P=1.34×10-2
P=1.89×10-2
P=7.94×10-6
P=5.32×10-4
P=1.75×10-2
P=2.91×10-2
P=9.60×10-4
b
A549 (WT) WCL
Vehicle
Cisplatin
siCon
siPITPα
siPITPβ
siPITPα+β
kDa
PI4,5P2
p53
PITPα
PITPβ
GAPDH
p53 levels
P=1.87×10-6
P=1.9×10-6
P=5.46×10-7
PI4,5P2
P=2.06×10-3
P=2.76×10-3
P=3.75×10-4
c
MDA-MB-231 (R280K)
Vehicle
Cisplatin
siCon
sip53
siPITPα
siPITPβ
siPITPα+β
siPITPNC1
kDa
PI4,5P2
p53
GAPDH
Merge
d
PI4,5P2
P=7.88×10-3
P=3.17×10-5
P=9.62×10-5
P=8.08×10-3
P=1.56×10-2
P=2.93×10-4
Vehicle
Cisplatin
e
A549 (WT) WCL
Vehicle
Cisplatin
siCon
siPITPα
siPITPβ
kDa
PI4P
PI4,5P2
PI3,4,5P3
PITPα
PITPβ
p53
GAPDH
f
PIPn level
Cis
PI4P
PI4,5P2
PI3,4,5P3
P=6.66×10-4
P=1.22×10-4
P=6.47×10-6
P=1.54×10-4
P=2.95×10-4
P=1.18×10-4
g
MDA-MB-231
siCon
siPITPα+β
Cis
kDa
PITPα
PITPβ
β-actin
Relative [3H]myo-inositol
Protein fraction
Gel homogenate
P=4.60×10-4
P=2.57×10-2

Fig. 6

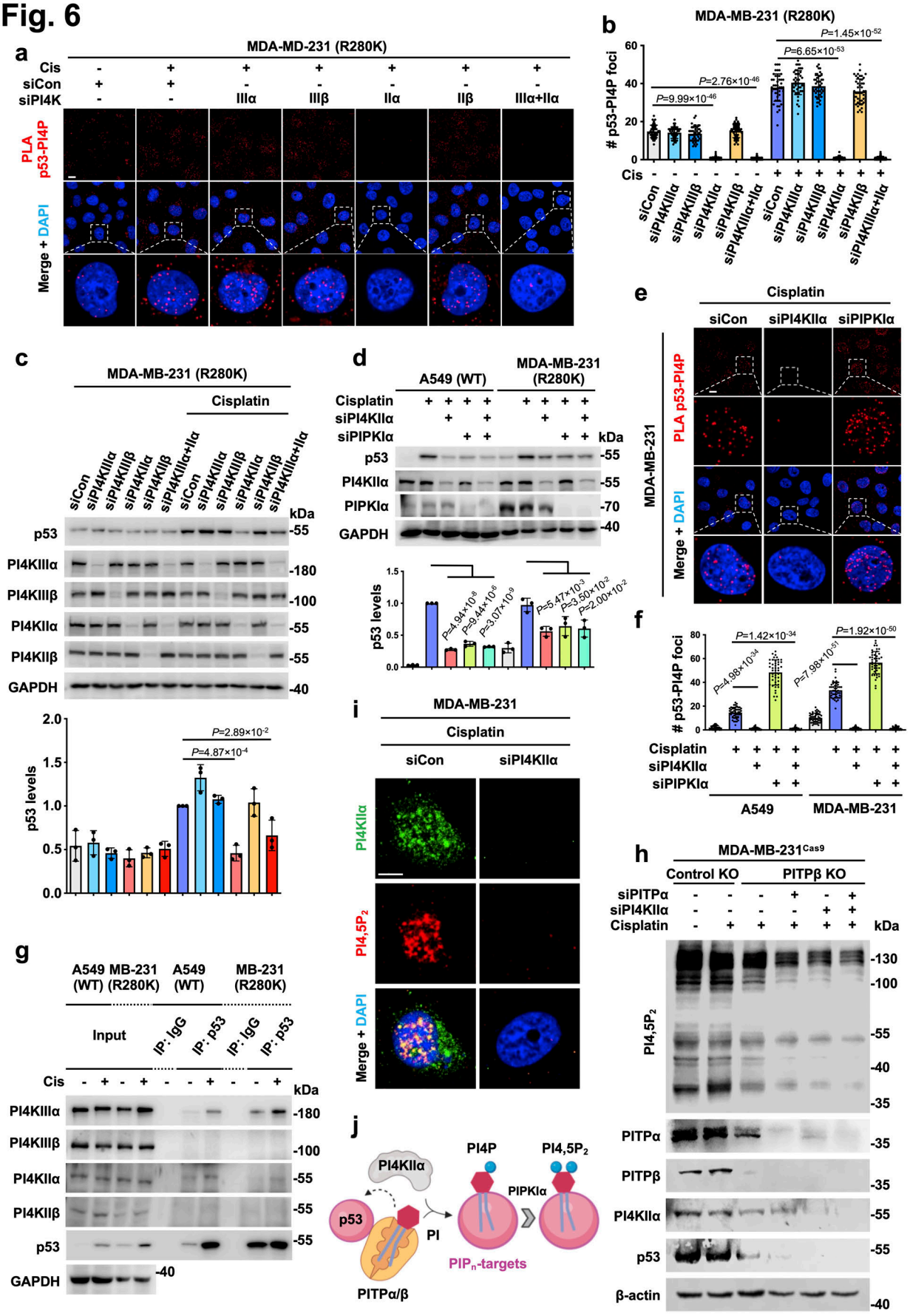
a
MDA-MD-231 (R280K)
Cis
siCon
siPI4K
IIIα
IIIβ
IIα
IIβ
IIIα+IIα
PLA p53-PI4P
Merge + DAPI
b
MDA-MB-231 (R280K)
# p53-PI4P foci
P=9.99×10-46
P=2.76×10-46
P=6.65×10-53
P=1.45×10-52
Cis
siCon
siPI4KIIIα
siPI4KIIIβ
siPI4KIIα
siPI4KIIβ
siPI4KIIIα+IIα
c
MDA-MB-231 (R280K)
Cisplatin
kDa
p53
PI4KIIIα
PI4KIIIβ
PI4KIIα
PI4KIIβ
GAPDH
p53 levels
P=4.87×10-4
P=2.89×10-2
d
A549 (WT)
MDA-MB-231 (R280K)
Cisplatin
siPI4KIIα
siPIPKIα
PIPKIα
P=4.94×10-8
P=9.44×10-6
P=3.07×10-9
P=5.47×10-3
P=3.50×10-2
P=2.00×10-2
e
Cisplatin
siCon
siPI4KIIα
siPIPKIα
MDA-MB-231
PLA p53-PI4P
Merge + DAPI
f
# p53-PI4P foci
P=4.98×10-34
P=1.42×10-34
P=7.98×10-51
P=1.92×10-50
A549
MDA-MB-231
g
A549 (WT)
MB-231 (R280K)
Input
IP: IgG
IP: p53
i
MDA-MB-231
Cisplatin
siCon
siPI4KIIα
PI4KIIα
PI4,5P2
Merge + DAPI
h
MDA-MB-231Cas9
Control KO
PITPβ KO
siPITPα
siPI4KIIα
Cisplatin
PI4,5P2
PITPα
PITPβ
β-actin
j
PI4KIIα
PI4P
PI4,5P2
PIPKIα
p53
PI
PIPn-targets
PITPα/β

Fig. 7

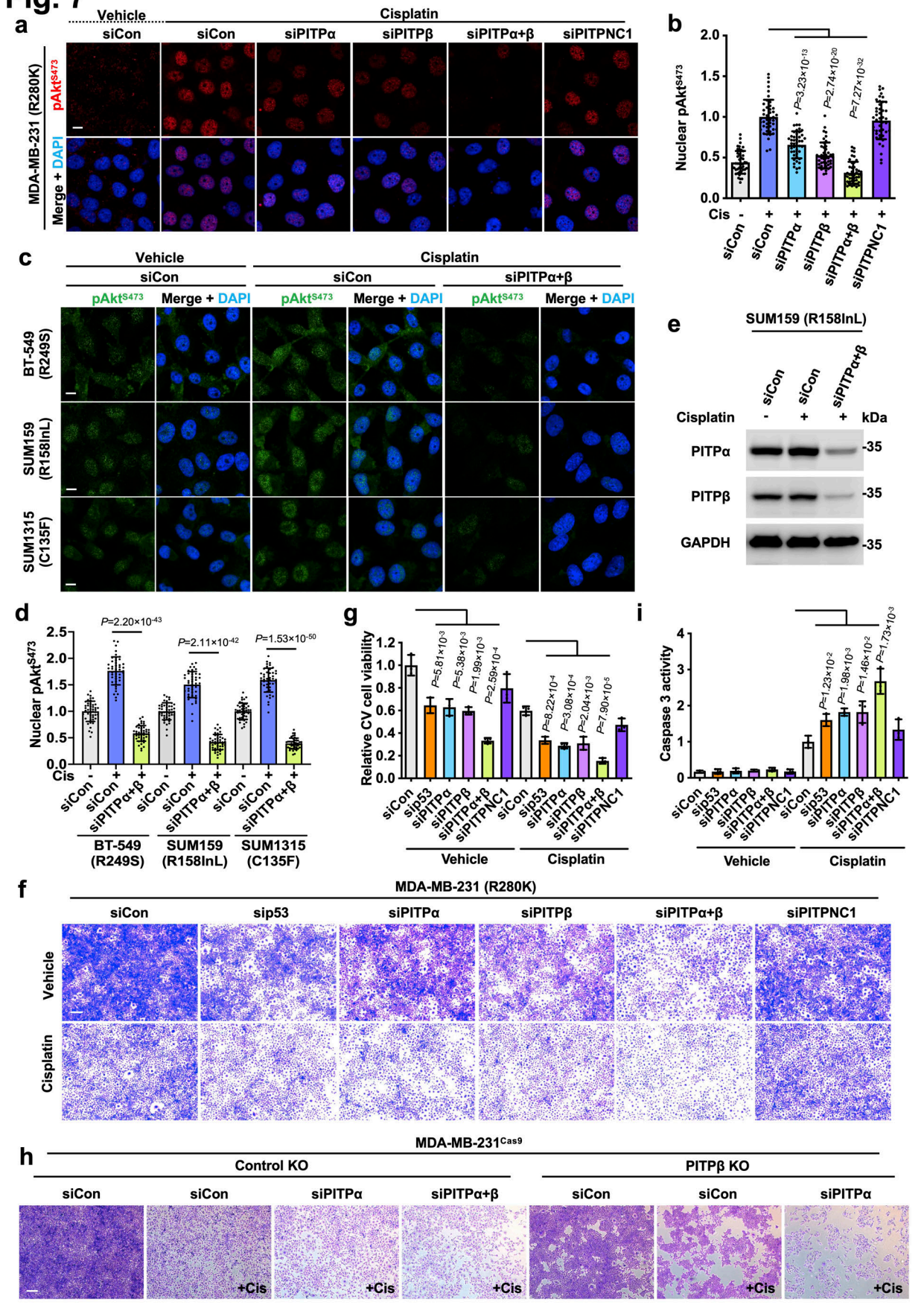
a
Vehicle
Cisplatin
siCon
siCon
siPITPα
siPITPβ
siPITPα+β
siPITPNC1
MDA-MB-231 (R280K)
pAkt S473
Merge + DAPI
b
Nuclear pAkt S473
P=3.23×10-13
P=2.74×10-20
P=7.27×10-32
Cis
siCon
siCon
siPITPα
siPITPβ
siPITPα+β
siPITPNC1
c
Vehicle
Cisplatin
siCon
siCon
siPITPα+β
pAkt S473
Merge + DAPI
BT-549 (R249S)
SUM159 (R158InL)
SUM1315 (C135F)
e
SUM159 (R158InL)
siCon
siCon
siPITPα+β
Cisplatin
kDa
PITPα
PITPβ
GAPDH
-35
d
P=2.20×10-43
P=2.11×10-42
P=1.53×10-50
Nuclear pAkt S473
Cis
BT-549 (R249S)
SUM159 (R158InL)
SUM1315 (C135F)
g
Relative CV cell viability
P=5.81×10-3
P=5.38×10-3
P=1.99×10-3
P=2.59×10-4
P=8.22×10-4
P=3.08×10-4
P=2.04×10-3
P=7.90×10-5
siCon
sip53
siPITPα
siPITPβ
siPITPα+β
siPITPNC1
Vehicle
Cisplatin
i
Caspase 3 activity
P=1.23×10-2
P=1.98×10-3
P=1.46×10-2
P=1.73×10-3
f
MDA-MB-231 (R280K)
siCon
sip53
siPITPα
siPITPβ
siPITPα+β
siPITPNC1
Vehicle
Cisplatin
h
MDA-MB-231Cas9
Control KO
PITPβ KO
siCon
siCon
siPITPα
siPITPα+β
siCon
siCon
siPITPα
+Cis

Fig. 8

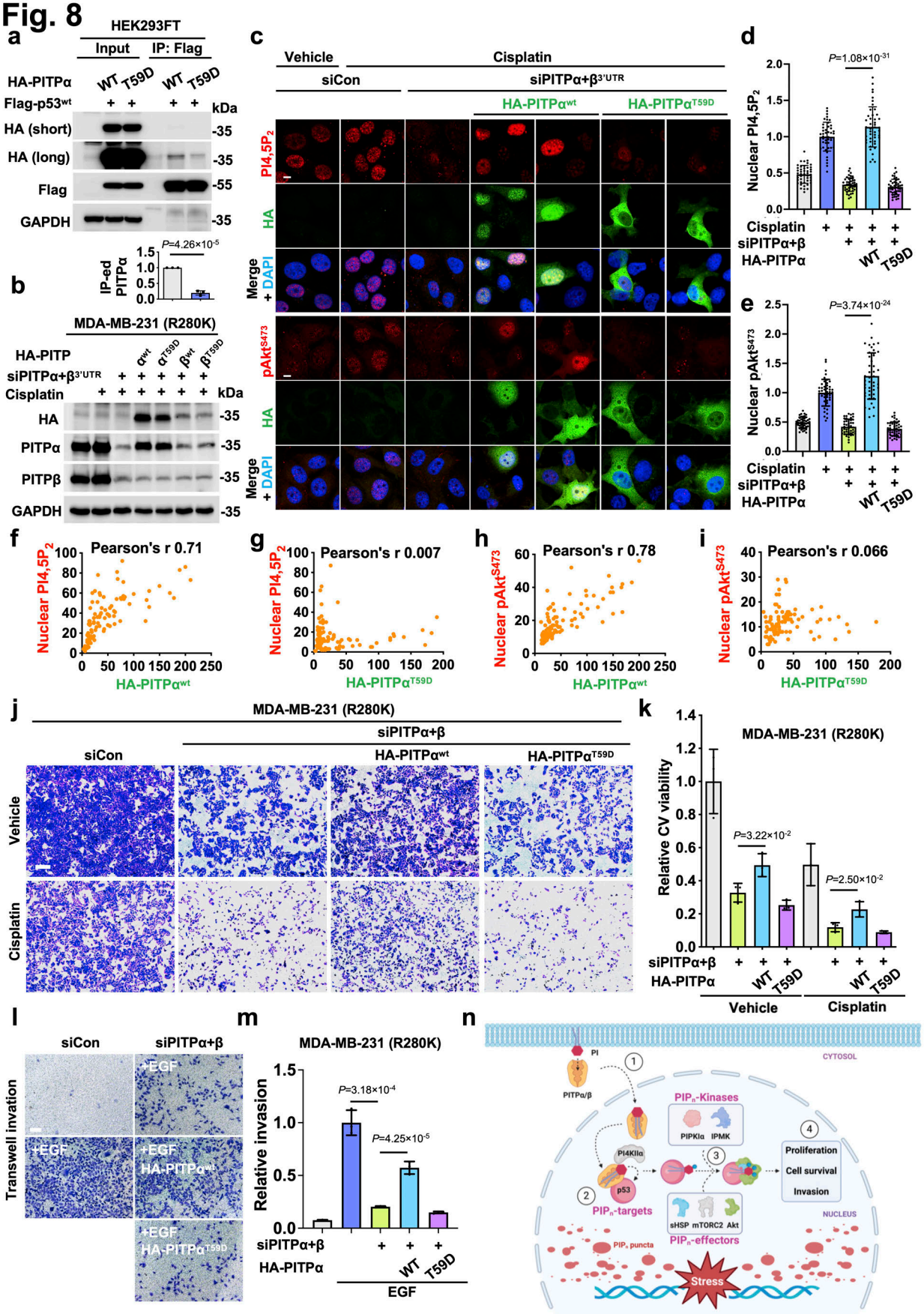
a
HEK293FT
Input
IP: Flag
HA-PITPα
WT
T59D
WT
T59D
Flag-p53wt
kDa
HA (short)
HA (long)
Flag
GAPDH
-35
-55
b
P=4.26×10-5
IP-ed PITPα
MDA-MB-231 (R280K)
HA-PITP
αwt
αT59D
βwt
βT59D
siPITPα+β3'UTR
Cisplatin
HA
PITPα
PITPβ
GAPDH
c
Vehicle
Cisplatin
siCon
siPITPα+β3'UTR
HA-PITPαwt
HA-PITPαT59D
PI4,5P2
HA
Merge + DAPI
pAktS473
d
P=1.08×10-31
Nuclear PI4,5P2
Cisplatin
siPITPα+β
HA-PITPα
WT
T59D
e
P=3.74×10-24
Nuclear pAktS473
f
Pearson's r 0.71
Nuclear PI4,5P2
HA-PITPαwt
g
Pearson's r 0.007
Nuclear PI4,5P2
HA-PITPαT59D
h
Pearson's r 0.78
Nuclear pAktS473
HA-PITPαwt
i
Pearson's r 0.066
Nuclear pAktS473
HA-PITPαT59D
j
MDA-MB-231 (R280K)
siPITPα+β
siCon
HA-PITPαwt
HA-PITPαT59D
Vehicle
Cisplatin
k
MDA-MB-231 (R280K)
Relative CV viability
P=3.22×10-2
P=2.50×10-2
siPITPα+β
HA-PITPα
WT
T59D
Vehicle
Cisplatin
l
siCon
siPITPα+β
Transwell invasion
+EGF
HA-PITPαwt
HA-PITPαT59D
m
MDA-MB-231 (R280K)
Relative invasion
P=3.18×10-4
P=4.25×10-5
siPITPα+β
HA-PITPα
WT
T59D
EGF
n
CYTOSOL
PI
PITPα/β
PIPn-Kinases
PIPKIα
IPMK
PI4KIIα
p53
PIPn-targets
sHSP
mTORC2
Akt
PIPn-effectors
PIPn puncta
Proliferation
Cell survival
Invasion
NUCLEUS
Stress

Extended Data Fig. 1

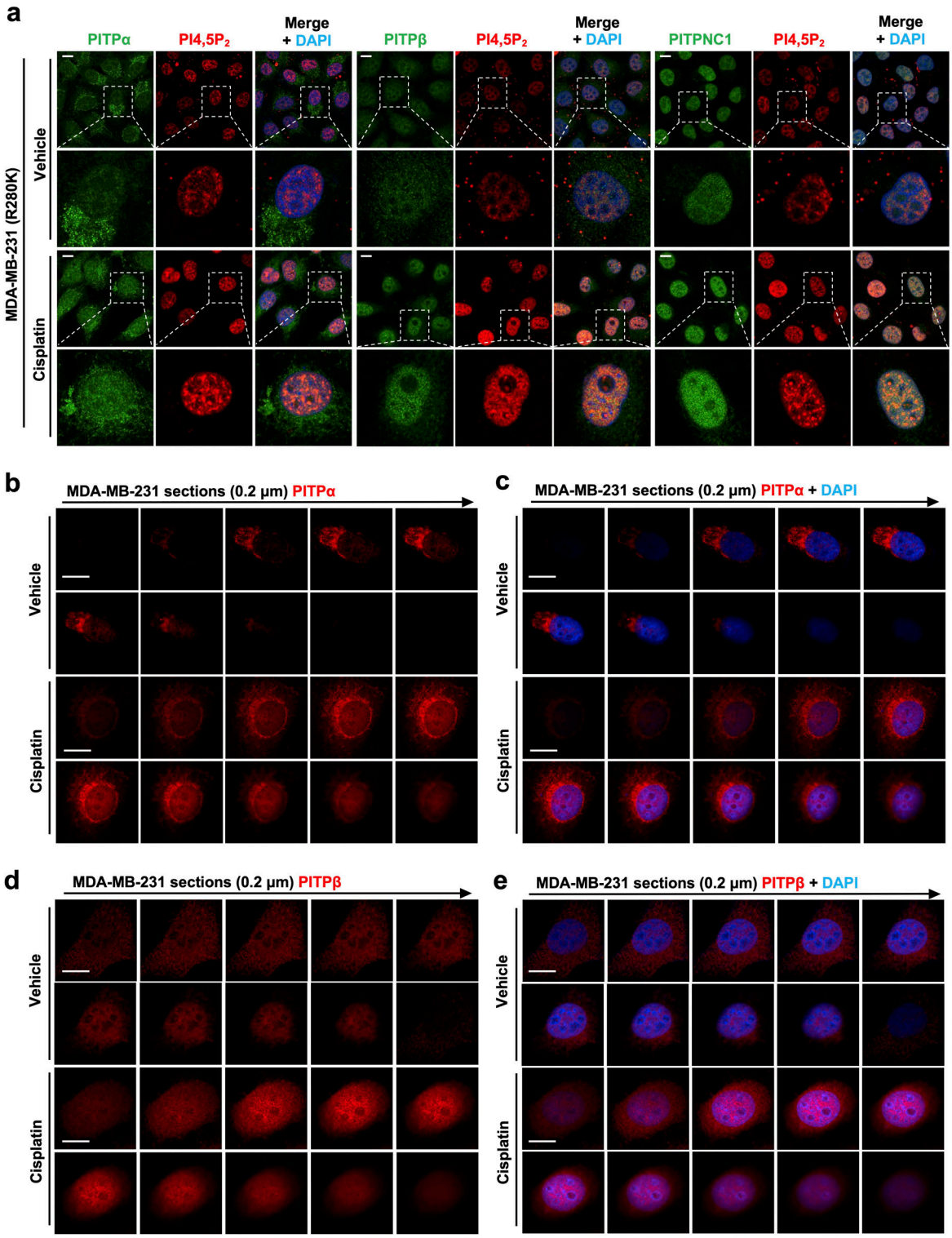

Extended Data Fig. 2

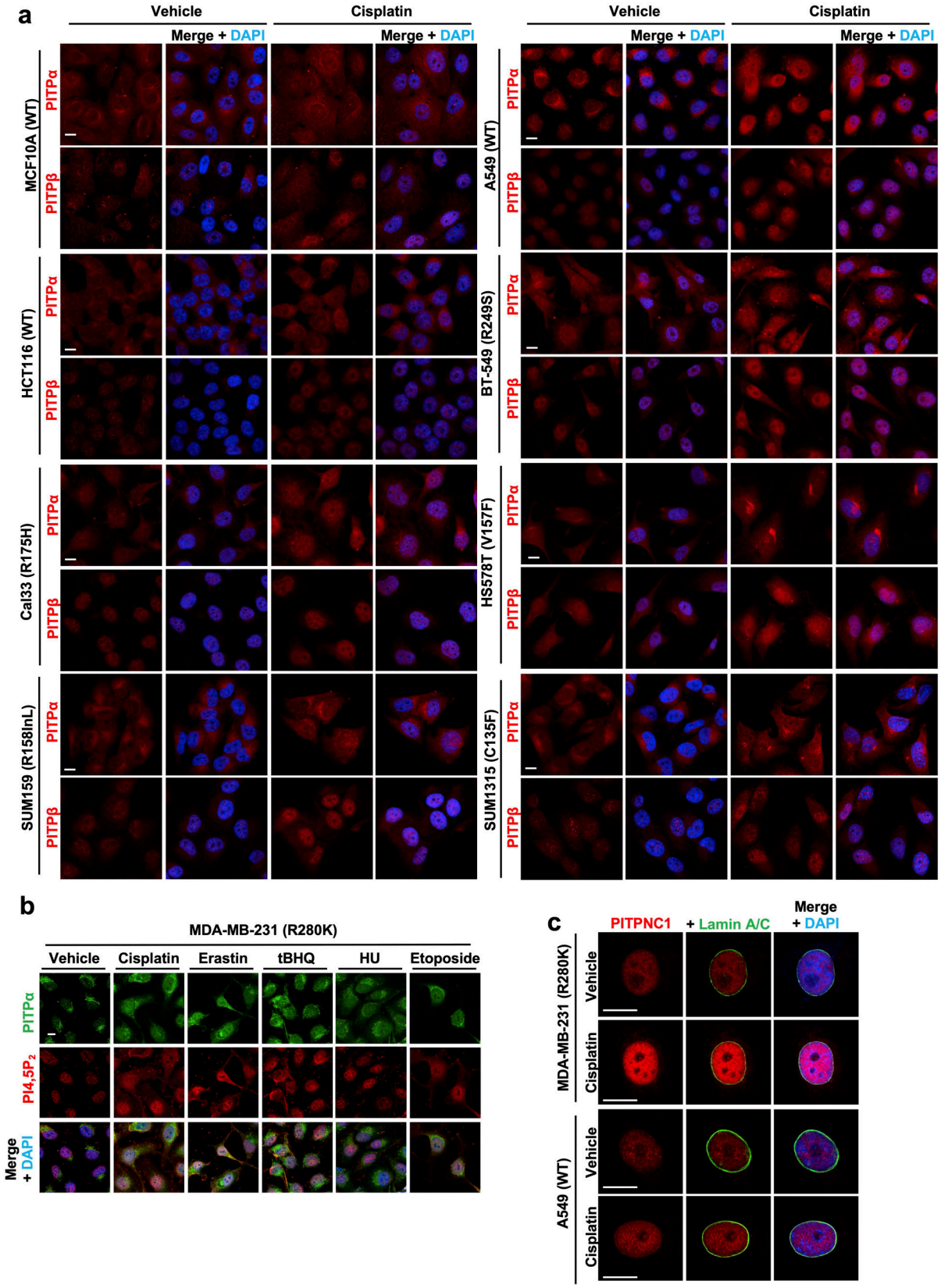

Extended Data Fig. 3

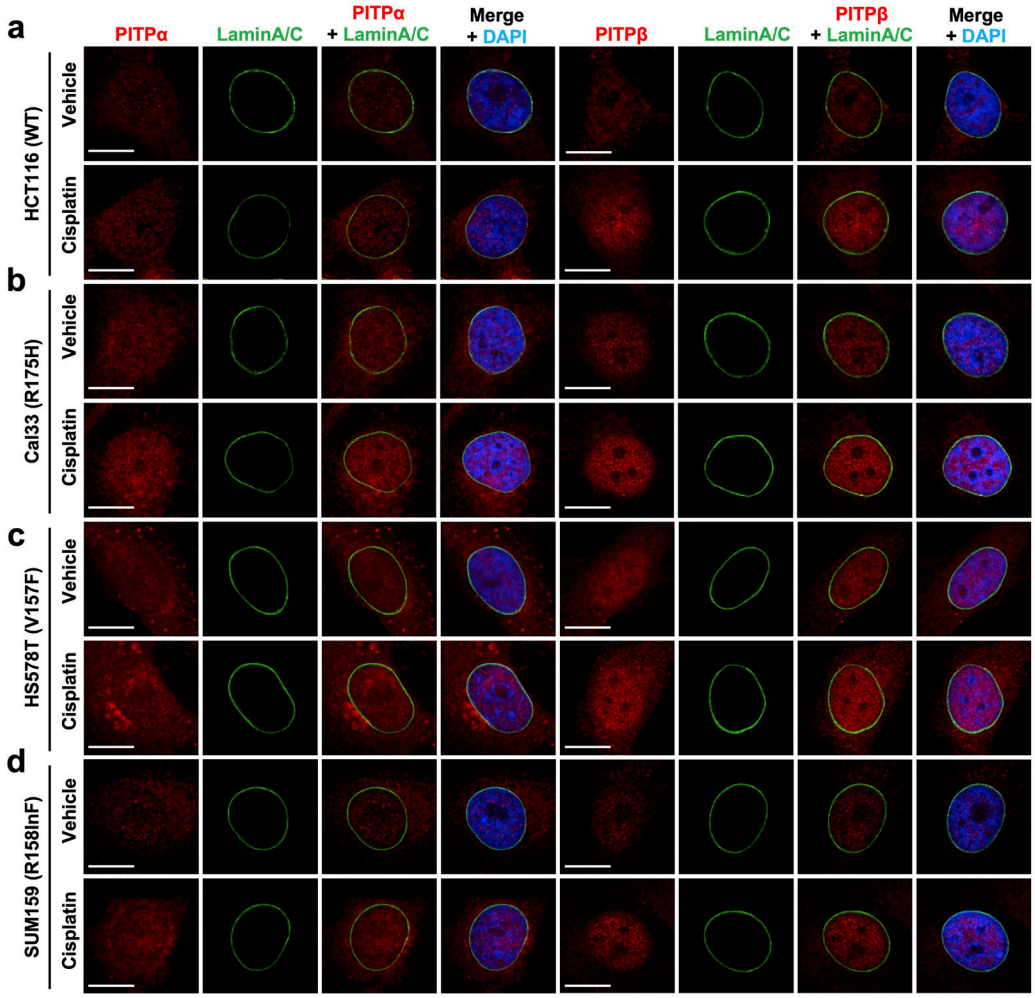

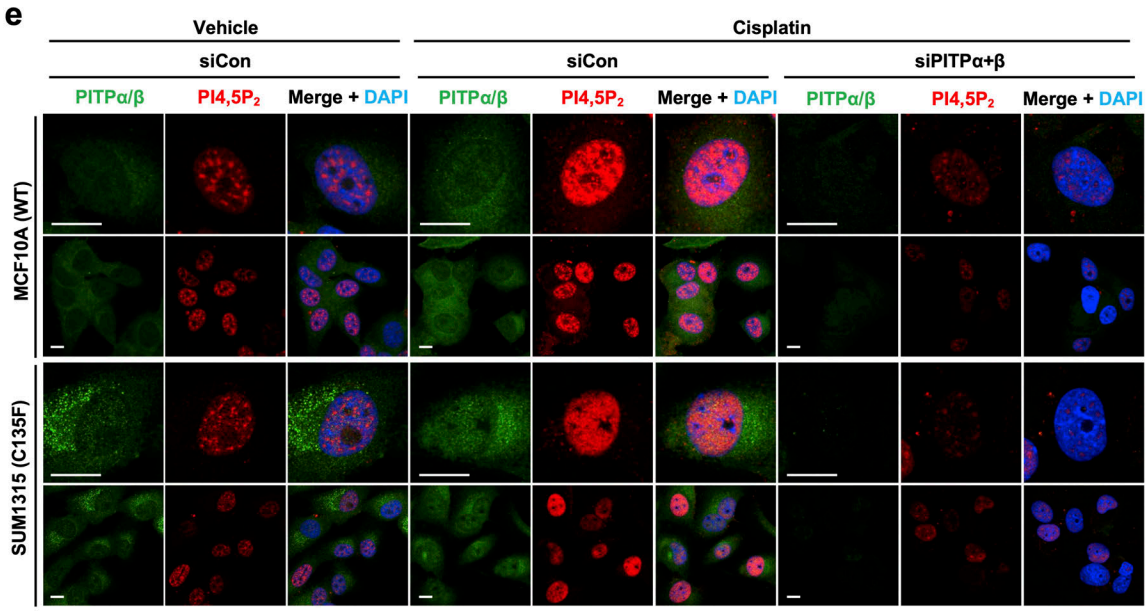

Extended Data Fig. 4

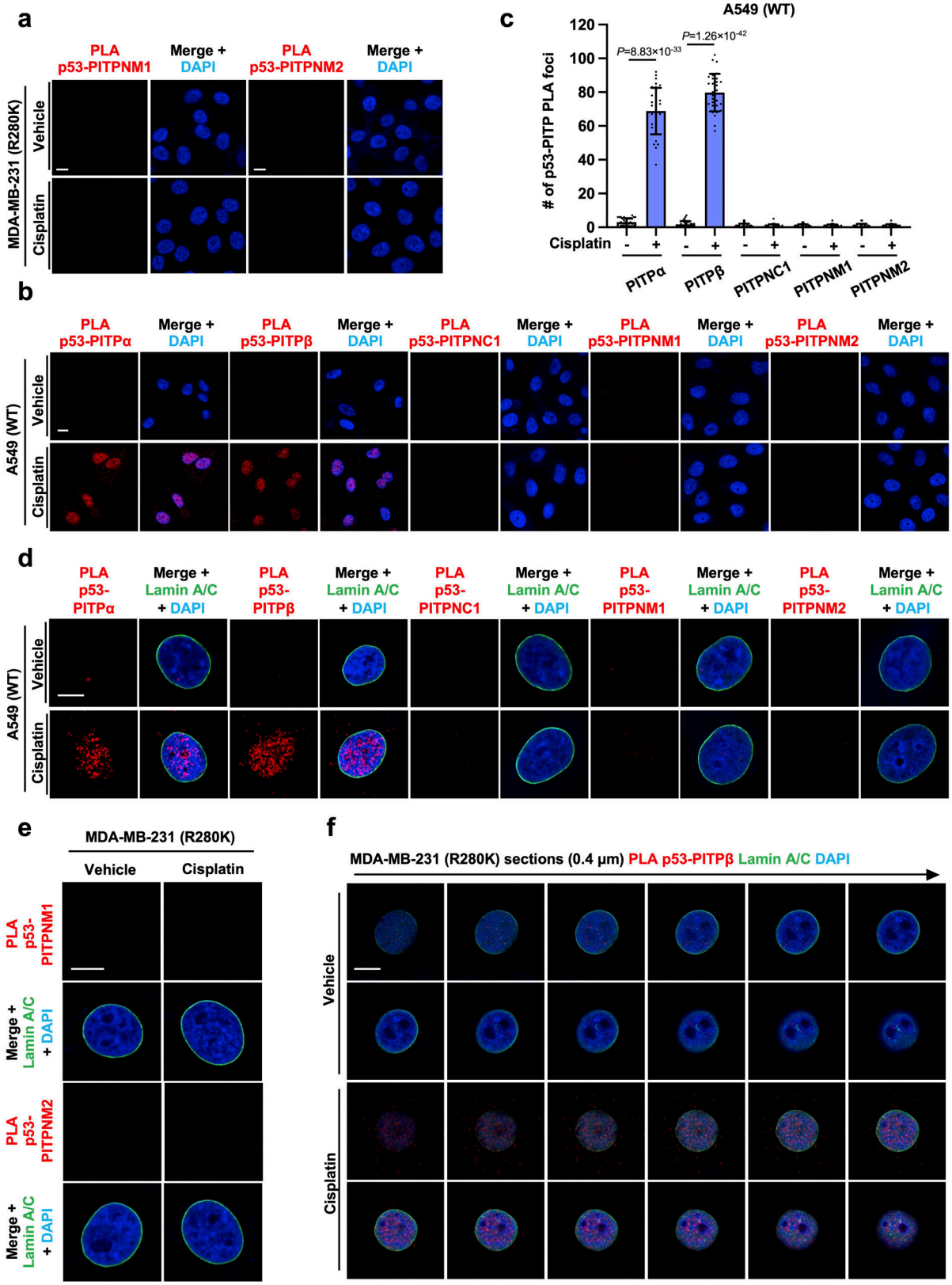

Extended Data Fig. 5

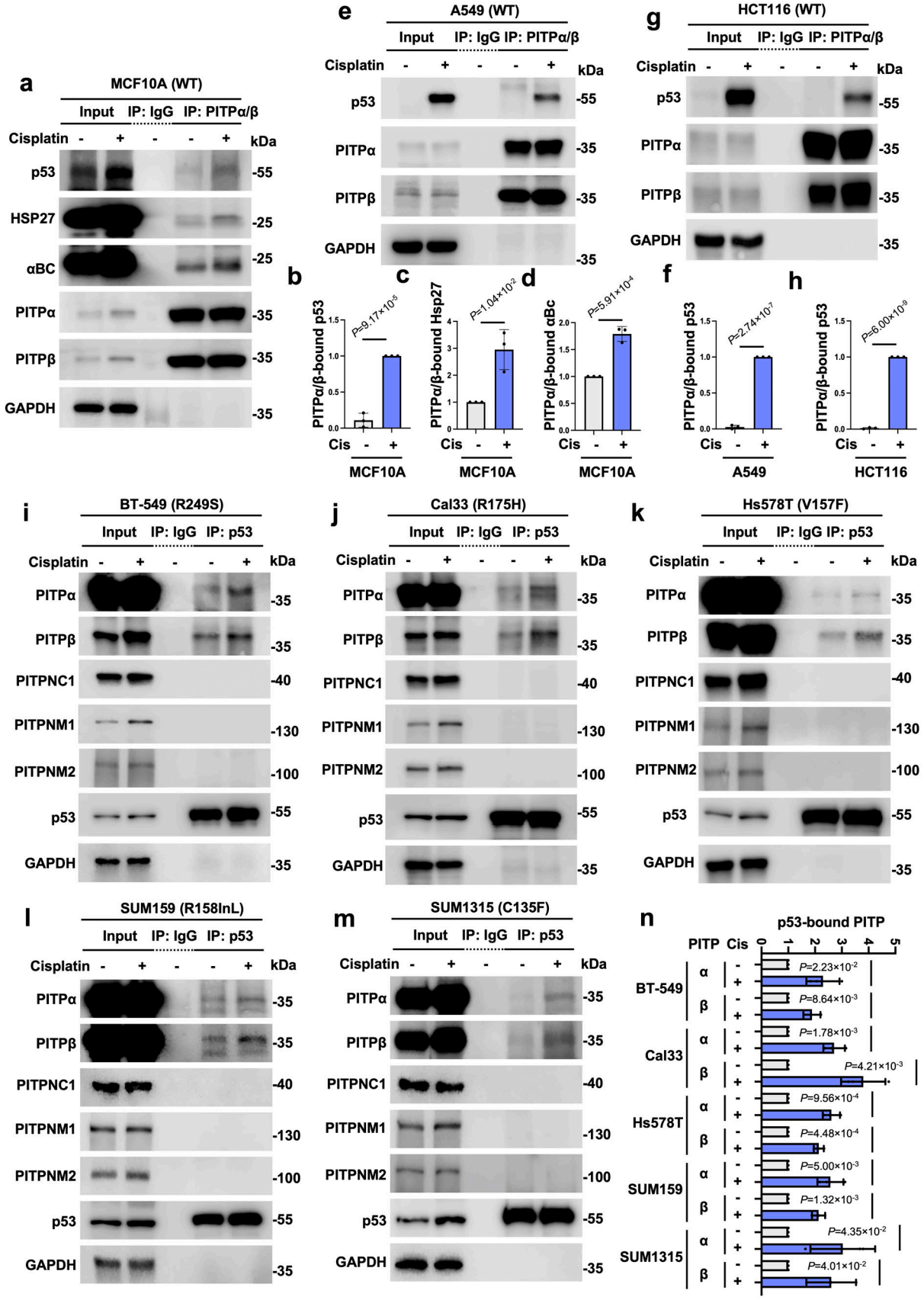

Extended Data Fig. 6

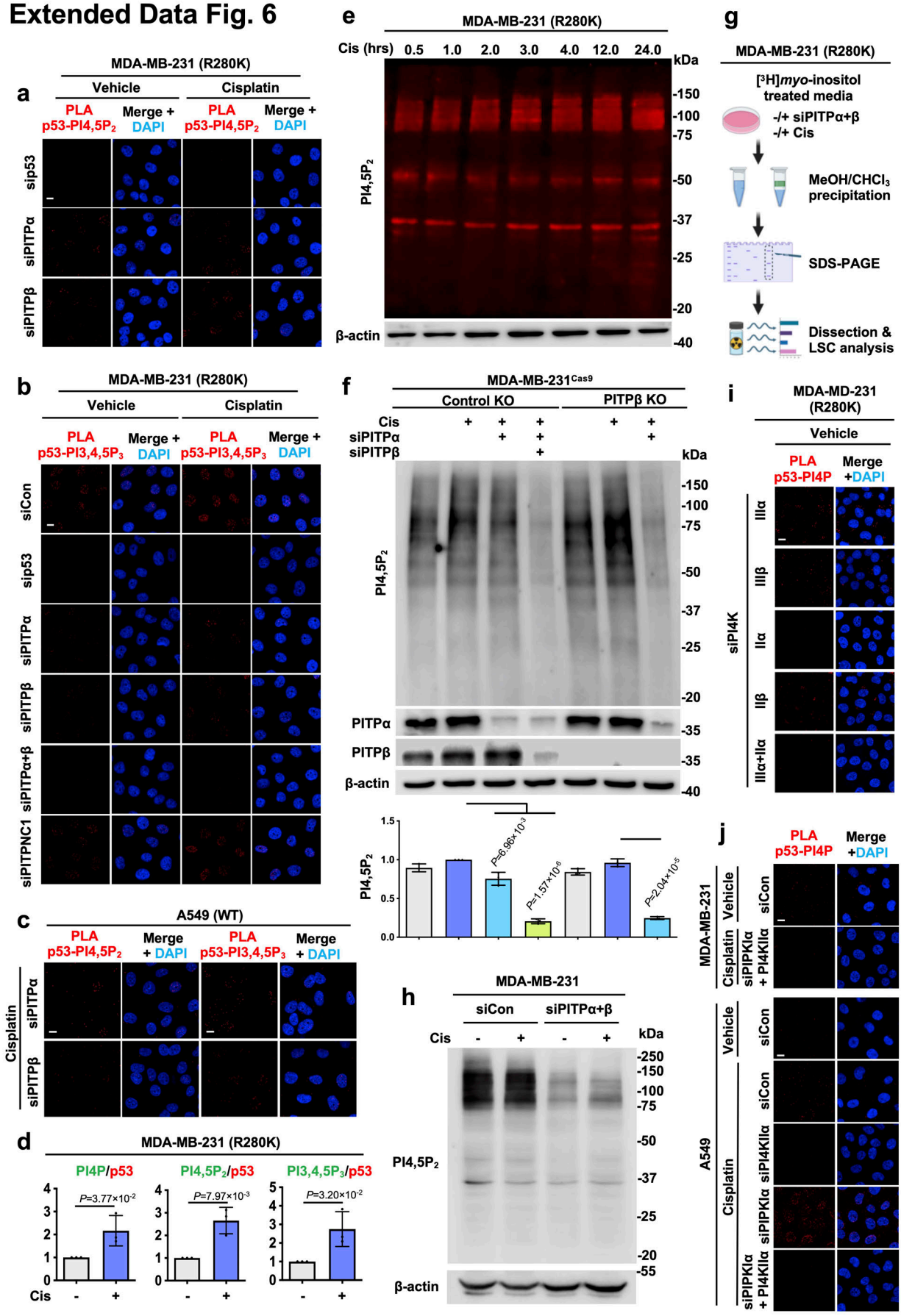

Extended Data Fig. 7

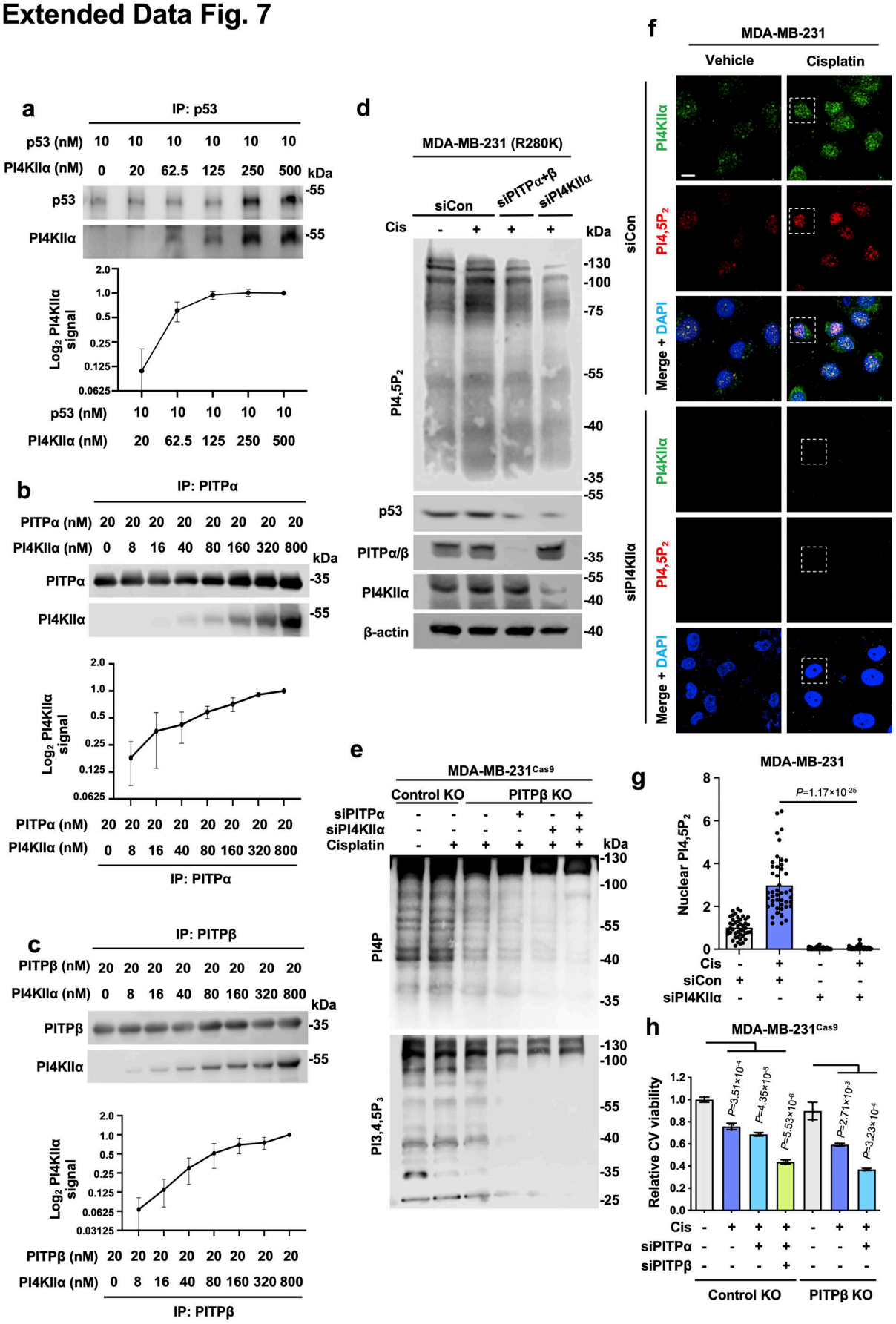

Extended Data Fig. 8

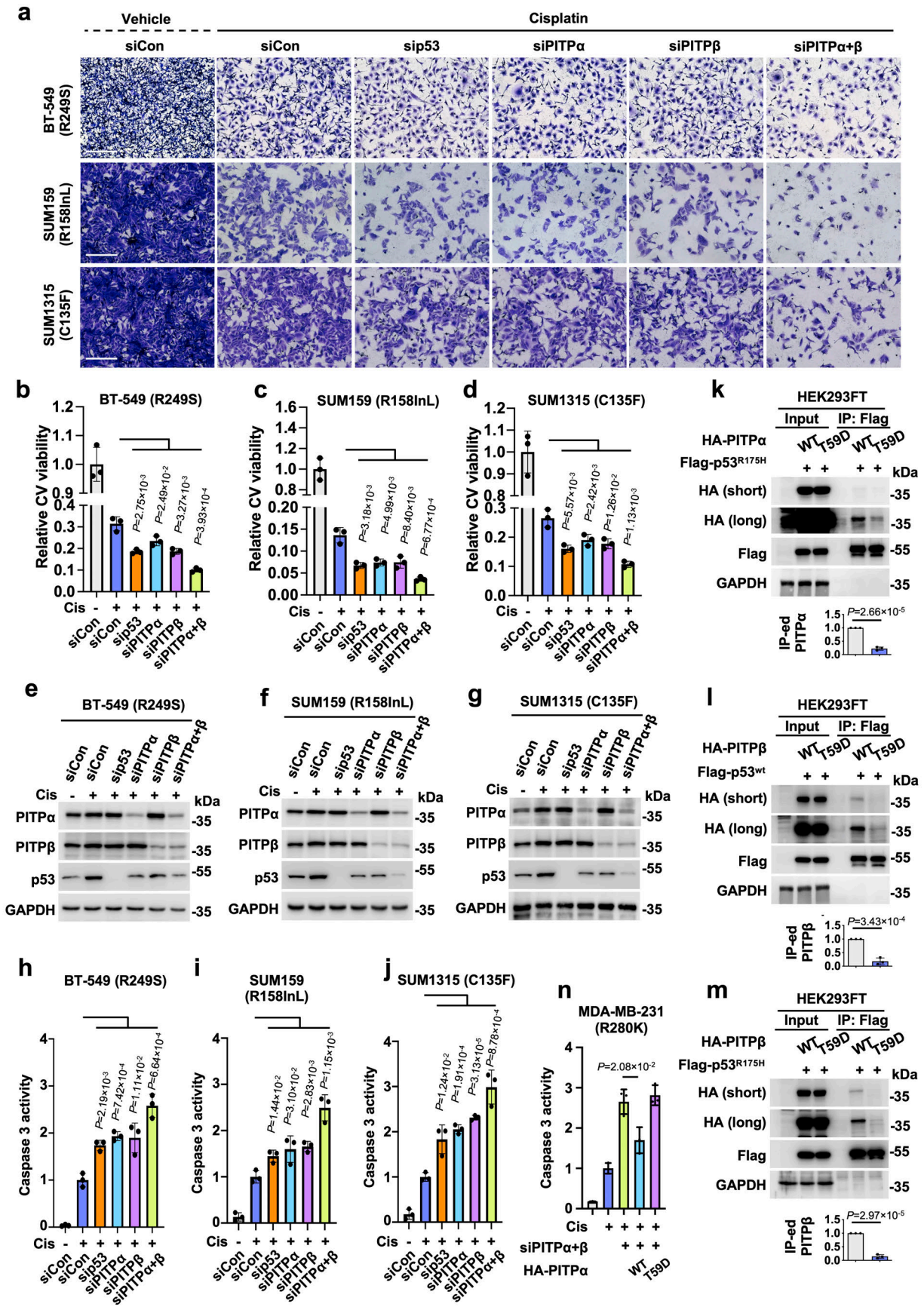

Click here to access/download
Supplemental Videos and Spreadsheets
Supplementary Video 1.mov

Click here to access/download
Supplemental Videos and Spreadsheets
Supplementary Video 2.mov